

AL/EQ-TR-1997-0044



## HIGH-TEMPERATURE HETEROGENEOUS REDOX CATALYSIS FOR NO<sub>x</sub> ABATEMENT

J. WHITE  
J. HEIDRICK  
S. ROARK  
J. MITCHEL  
A. F. SAMMELLS  
ELTRON RESEARCH, INC.  
5660 AIRPORT BOULEVARD  
BOULDER CO 80301-2340

23 JANUARY 1998

FINAL REPORT: 25 APR 97 – 25 OCT 97

Approved for public release; distribution unlimited

AIR FORCE RESEARCH LABORATORY  
MATERIALS & MANUFACTURING DIRECTORATE  
AIRBASE & ENVIRONMENTAL TECHNOLOGY DIVISION  
TYNDALL AFB FL 32403-5323

19980521 006


DTIC QUALITY INSPECTED 4

## NOTICES


WHEN GOVERNMENT DRAWINGS, SPECIFICATIONS, OR OTHER DATA INCLUDED IN THIS DOCUMENT FOR ANY PURPOSE OTHER THAN GOVERNMENT PROCUREMENT DOES NOT IN ANYWAY OBLIGATE THE US GOVERNMENT. THE FACT THAT THE GOVERNMENT FORMULATED OR SUPPLIED THE DRAWINGS, SPECIFICATIONS, OR OTHER DATA, DOES NOT LICENSE THE HOLDER OR ANY OTHER PERSON OR CORPORATION; OR CONVEY ANY RIGHTS OR PERMISSION TO MANUFACTURE, USE, OR SELL ANY PATENTED INVENTION THAT MAY RELATE TO THEM.

THIS REPORT IS RELEASABLE TO THE NATIONAL TECHNICAL INFORMATION SERVICE (NTIS). AT NTIS, IT WILL BE AVAILABLE TO THE GENERAL PUBLIC, INCLUDING FOREIGN NATIONS.


THIS TECHNICAL REPORT HAS BEEN REVIEWED AND IS APPROVED FOR PUBLICATION.



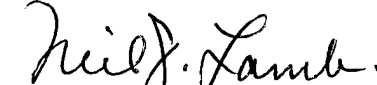
**JOSEPH D. WANDER, PhD**  
Program Manager



**ALLAN M. WEINER, Lt Col, USAF**  
Chief, Environmental Technology  
Development Branch



**ANDREW D. POULIS**  
Scientific & Technical  
Information Program Manager



**NEIL J. LAMB, Col, USAF, BSC**  
Chief, Airbase & Environmental  
Technology Division

IF YOUR ADDRESS HAS CHANGED, IF YOU WISH TO BE REMOVED FROM OUR MAILING LIST, OR IF THE ADDRESSEE IS NO LONGER EMPLOYED BY YOUR ORGANIZATION, PLEASE NOTIFY AFRL/MLQC, TYNDALL AFB FLORIDA 32403-5323, TO HELP MAINTAIN A CURRENT MAILING LIST.

Do not return copies of this report unless contractual obligations or notice on a specific document requires its return.

REPORT DOCUMENTATION PAGE			Form Approved OMB No. 0704-0188	
<small>Public reporting burden for this collection of information is estimated to average 1 hour per response, including the time for reviewing instructions, searching existing data sources, gathering and maintaining the data needed, and completing and reviewing the collection of information. Send comments regarding this burden estimate or any other aspect of this collection of information, including suggestions for reducing this burden, to Washington Headquarters Services, Directorate for Information Operations and Reports, 1215 Jefferson Davis Highway, Suite 1204, Arlington, VA 22202-4302, and to the Office of Management and Budget, Paperwork Reduction Project (0704-0188), Washington, DC 20503.</small>				
1. AGENCY USE ONLY (Leave Blank)		2. REPORT DATE January 23, 1998	3. REPORT TYPE AND DATES COVERED Final Report 4/25/97 to 10/25/97	
4. TITLE AND SUBTITLE High-Temperature Heterogeneous Redox Catalysis for NO <sub>x</sub> Abatement			5. FUNDING NUMBERS C: F41624-97-C-0010 PE: 65502F Project: 3005 WU:	
6. AUTHOR(S) J. White, J. Heidrick. S. Roark, J. Mitchel and A.F. Sammells				
7. PERFORMING ORGANIZATION NAME(S) AND ADDRESS(ES) Eltron Research, Inc. 5660 Airport Boulevard Boulder, CO 80301-2340			8. PERFORMING ORGANIZATION REPORT NUMBER	
9. SPONSORING/MONITORING AGENCY NAME(S) AND ADDRESS(ES) Armstrong Laboratory Environics Directorate Environmental Risk Reduction Technologies Division Attn: Dr. Joseph D. Wander 139 Barnes Drive, Suite 2 Tyndall AFB, FL 32403-5323			10. SPONSORING/MONITORING AGENCY REPORT NUMBER AL/EQ-TR-1997-0044	
11. SUPPLEMENTARY NOTES				
12a. DISTRIBUTION/AVAILABILITY STATEMENT Unlimited Distribution			12b. DISTRIBUTION CODE A	
13. ABSTRACT (Maximum 200 words)  This Phase I SBIR program was directed towards the synthesis, characterization, and determination of preferred catalyst compositions for the high-temperature direct (reagentless) decomposition of nitrogen oxides in exhaust streams. Phase I results showed clearly that significant persistent (nontransient) activity (35% removal) for direct deNO <sub>x</sub> (at > 500°C) could be attained in helium at space velocities of ~1,000,000 h <sup>-1</sup> (3.6ms residence time) over a brownmillerite catalyst supported on a powdered ceramic (yttria-stabilized zirconia) representative of thermal barrier coatings, in the presence of 16% O <sub>2</sub> , absent of any reagent. This catalyst, when unsupported, showed persistent activity (27% removal at 500,000h <sup>-1</sup> for at least 6 hours and at least 140 hours at 50,000 h <sup>-1</sup> ). Significant activity was measured at up to 1,000°C. These catalysts also possessed exceptional activity for the combustion of propane and propylene as well as measurable activity for oxidation of CO. Preliminary results showed tolerance to feedstream CO <sub>2</sub> (10%) and SO <sub>2</sub> (10ppm). Results point clearly to probable attainment of Air Force's Phase II targets of 50% removal in millisecond residence time regimes and retention of 50% of initial activity after 500 hours.				
14. SUBJECT TERMS Redox Catalysts, Nitrogen Oxides, Exhausts, High Temperature			15. NUMBER OF PAGES	
			16. PRICE CODE	
17. SECURITY CLASSIFICATION OF REPORT Unclassified	18. SECURITY CLASSIFICATION OF THIS PAGE Unclassified	19. SECURITY CLASSIFICATION OF ABSTRACT Unclassified	20. LIMITATION OF ABSTRACT UL	

## EXECUTIVE SUMMARY

### A. OBJECTIVE

The objective of this research project was to evaluate new catalysts for achieving the high rate decomposition of nitrogen oxides under conditions representative of those encountered in the exhausts of gas turbines such as air breathing propulsion systems (jet engines). This subject is of importance to the Air Force in several respects, including the reduction of the chemical signatures of jet propelled aircraft and emissions reduction in stationary sources of  $\text{NO}_x$ .

### B. BACKGROUND

The emission of nitrogen oxides and incompletely oxidized species (unburned hydrocarbons and carbon monoxide) is of concern to the Air Force in at least two respects: 1) the chemical signature produced by jet propelled aircraft and 2) the environmental effects of stationary sources at Air Force installations, including jet engine test cells, and the possibility of their future regulation. Resolution of the first problem will likely lead to a solution to the second, as the severity of conditions encountered in gas turbine exhausts are anticipated to require approaches and materials possessing remarkable attributes.

### C. SCOPE

This report describes research done under the DoD Small Business Innovation Research (SBIR) program, Contract No. F41624-97-C-0010, "High-Temperature Heterogeneous Redox Catalysis for  $\text{NO}_x$  Abatement." The impetus for the program comes from the need to reduce the chemical signatures of jet propelled aircraft in the Air Force combat inventory. Methods currently available are insufficient for this purpose. Particularly troublesome is the nature of gas turbine exhausts: extremely high (> 15 percent) levels of oxygen, which tend to poison catalysts, are encountered in these sources. Catalytic approaches have, until the present, failed under these conditions. Results presented in the report indicate that this barrier has been overcome and that a reagentless catalysis system for  $\text{deNO}_x$  of gas streams is now available.

### D. METHODOLOGY

Catalyst candidates were chosen on the basis of anticipated metal - oxygen binding energies, transition-metal electronic configuration, and anticipated acid-base properties. The experimental protocol consisted of coarse screening a number of candidates possessing a range of the aforementioned properties and selecting the most active candidates for subsequent modification. Screening of these modifications led to the selection of a number of candidates for further study. The experimental apparatus used was Eltron's catalyst test stand, which consists of six reactors. Gases to each reactor were supplied by stainless steel and aluminum conduit, controlled by precision metering valves, and measured using Gilmont flow meters. Measurements of nitrogen oxides and products of their decomposition were performed using a Leybold - Inficon residual gas analyzer (RGA) equipped with a quadrupole mass spectrometer. Measurement of  $\text{NO}_x$

was also performed using City Technology electrochemical NO and NO<sub>2</sub> sensors.

## E. TEST DESCRIPTION

Experiments consisted of introducing into a heated reactor containing catalyst powder or monolith supported catalyst, a simulated exhaust stream containing nitric oxide (NO) at concentrations of 370 - 1000 ppm, oxygen at 0 - 16 percent, and a balance of helium. Preferred catalysts were also exposed to a gas mixture containing, in addition to the aforementioned gases, 10 percent CO<sub>2</sub> and 10 ppm SO<sub>2</sub>. Analysis of the reactor inlet stream, as well as effluent, was conducted for each experiment. The influence of the variation of oxygen concentration, temperature, and on line time was conducted for preferred catalysts.

## F. RESULTS

Removal of up to 91 percent of NO in 16 percent O<sub>2</sub> at 50,000 h<sup>-1</sup> and 400°C was observed over the best catalyst examined. The same catalyst, when supported on yttria-stabilized zirconia (YSZ) removed 35% of 477 ppm NO in 16 percent O<sub>2</sub> at 500°C and a space velocity of 1,000,000 h<sup>-1</sup>. In neither of these cases was a reductant necessary to obtain this activity. To our knowledge, these catalysts constitute the only materials extant which possess reagentless activity under these conditions.

## G. CONCLUSIONS

Catalysts developed during this program have demonstrated practical activities for gas turbine applications. Application in millisecond residence time regimes has been shown to be possible. The catalysts developed during the program possess compatibility with thermal barrier coating (TBC) materials. In addition, the materials can be deposited on high temperature alloy surfaces using Eltron's reactive plasma surfacing technology. As a consequence, it will be possible to reduce jet engine emissions without pressure drop by incorporating the catalyst onto hot engine surfaces, such as the expander stator or the nozzle lining.

## H. RECOMMENDATIONS

The catalyst compositions developed thus far must be optimized for operation in specific systems. The development of catalyst application procedures is necessary for employment in jet propulsion systems. Furthermore, testing at the relevant scale is essential. For example, a monolith incorporating the preferred catalyst could be mounted inside of a jet engine test cell or burn rig capable of simulating combustion conditions from a jet engine.

## TABLE OF CONTENTS

	<u>Page</u>
I. INTRODUCTION	1
A. Objective	1
B. Program Background	1
C. Scope	2
II. PHASE I TECHNICAL OBJECTIVES	3
III. WORK PERFORMED AND RESULTS OBTAINED	4
Task 1 Performance Testing of Redox Catalysts for NO <sub>x</sub> Decomposition	4
A. Synthesis of Catalysts	4
B. Catalyst Testing	5
Task 2 Optimization of Catalysts	13
A. Analysis	17
B. Catalyst Performance	18
Task 3 Selection and Performance Testing of Supported Catalysts	32
IV. SUMMARY OF FINDINGS DURING PHASE I	35
V. ESTIMATES OF TECHNICAL FEASIBILITY	37
A) Anticipated Results	37
B) Potential Use by Government	37
C) Potential Commercial Applications	38
D) Significance of Anticipated Results with Regard to Phase III	38
VI. REFERENCES	38

## LIST OF FIGURES

	<u>Page</u>
Figure 1. Schematic of catalyst mechanistic features of approach for promoting NO <sub>x</sub> decomposition.	1
Figure 2. Decision tree used during Phase I for selection of preferred NO <sub>x</sub> decomposition catalysts.	2
Figure 3. Photograph of Catalyst Test Stand Used to Characterize the Performance of DeNO <sub>x</sub> Catalysts.	8
Figure 4. Schematic of dual reactor system incorporating a quadrupole mass spectrometer for study of high temperature NO <sub>x</sub> decomposition under net oxidizing conditions.	9
Figure 5. Plot of %NO removed at 750°C and 3200 h <sup>-1</sup> over bismuth tungstate catalysts in Table 3.	11
Figure 6. X-Ray diffraction pattern of Catalysts 2a and 2b synthesized respectively A) from oxides and B) by coprecipitation.	12
Figure 7. Partial pressure data determined by mass spectroscopy for removal of nitrogen oxide (500ppm) from a stream 16% in O <sub>2</sub> over Catalyst 2b. T=500°C.	14
Figure 8. Schematic of the GC 10-port sampling valve.	18
Figure 9. Plot of NO decomposed over Catalyst 102 versus temperature. GHSV = 50,000 h <sup>-1</sup> . 1000 ppm NO, 16% O <sub>2</sub> .	19
Figure 10. Plot of NO decomposed over Catalyst 102 versus space velocity for 1000 ppm NO in 16% O <sub>2</sub> . 1000 ppm CO. T=1000°C.	19
Figure 11. Plot of NO decomposed over Catalyst 102 versus space velocity for 1000 ppm NO, 16% O <sub>2</sub> . T=500°C.	20
Figure 12. X-ray diffraction pattern of Catalyst 102 prepared by calcination of oxides at 1000°C for 4 hours.	21
Figure 13. X-ray diffraction pattern of Catalyst 102 after 18.5 hours online.	21

## LIST OF FIGURES (Continued)

	<u>Page</u>
Figure 14. XRD pattern of Catalyst 104 prepared from the oxides.	22
Figure 15. NO decomposed over Catalyst 104 versus temperature. 1000ppm NO, 16%O <sub>2</sub> . GHSV = 50,000 h <sup>-1</sup> .	22
Figure 16. NO decomposed over Catalyst 104 versus space velocity. T=500°C. 1000 ppm NO, 16% O <sub>2</sub> .	23
Figure 17. XRD pattern of Catalyst 104 after 4.5 hours on line.	23
Figure 18. XRD pattern of Catalyst 105 prepared by calcination of metal oxides at 1000°C.	25
Figure 19. XRD pattern of Catalyst 105 after 1.5 hours on line.	25
Figure 20. NO decomposition versus temperature for Catalyst 105. GHSV = 50,000 h <sup>-1</sup> . 1000 ppm NO, 16% O <sub>2</sub> .	26
Figure 21. NO decomposed <u>versus</u> space velocity for Catalyst 105. T=1000°C. 1000 ppm NO. 16% O <sub>2</sub> . 1000 ppm CO.	26
Figure 22. NO decomposed over Catalyst 105 versus GHSV. T=500°C. 1000 ppm NO, 16% O <sub>2</sub> .	27
Figure 23. Plot of deNO <sub>x</sub> activity of Catalyst 105 versus temperature. GHSV = 50,000 h <sup>-1</sup> . 1000 ppm NO, 16% O <sub>2</sub> .	27
Figure 24. Plot of NO decomposed over Catalyst 105 versus oxygen content of stream. T=500°C. GHSV=50,000 h <sup>-1</sup> . No reductant was present in the feed.	29
Figure 25. NO decomposed over Catalyst 105 as a function of NO concentration. T=500°C. 16% O <sub>2</sub> . GHSV=50,000 h <sup>-1</sup> . No reductant was present in the feed.	29
Figure 26. Plot of deNO <sub>x</sub> activity for Catalyst 105 versus time on line. T=500°C. GHSV=50,000 h <sup>-1</sup> . 1000 ppm NO, 16% O <sub>2</sub> .	30
Figure 27. Plot of deNO <sub>x</sub> activity for Catalyst 105 versus time on line. GHSV = 500,000 h <sup>-1</sup> . 1000 ppm NO, 16% O <sub>2</sub> .	30

## LIST OF FIGURES (Continued)

	<u>Page</u>
Figure 28.	Plot of $\text{deNO}_x$ over Catalyst 105 (4.3 wt%/YSZ) versus space velocity. NO concentration: 1000 ppm up to 250,000 $\text{h}^{-1}$ , 953 ppm at 500,000 $\text{h}^{-1}$ , 636 ppm at 750,000 $\text{h}^{-1}$ , and 477 ppm at 1,000,000 $\text{h}^{-1}$ . 16% $\text{O}_2$ . BET surface area = 2.5 $\text{m}^2/\text{g}$ . Weight catalyst used: 0.025g.
	33
Figure 29.	Plot of NO conversion versus time online for Catalyst 98 (3.2wt%)/YSZ. $T = 500^\circ\text{C}$ . 1000 ppm NO, 16% $\text{O}_2$ . GHSV = 50,000 $\text{h}^{-1}$ .
	34
Figure 30.	NO decomposed versus time for Catalyst 98 (0.313g) supported on 1cm long, 1cm diameter Cordierite monolith. $T = 500^\circ\text{C}$ . 1000 ppm NO, 16% $\text{O}_2$ . GHSV = 15,000 $\text{h}^{-1}$ .
	34
Figure 31.	NO decomposed versus space velocity for Catalyst 105 (loading: 0.027g)/cordierite monolith. $T = 500^\circ\text{C}$ . NO concentration: 1000 ppm for 10,000 and 25,000 $\text{h}^{-1}$ , 625 ppm for 40,000 $\text{h}^{-1}$ , and 500 ppm for 50,000 $\text{h}^{-1}$ . 16% $\text{O}_2$ .
	35

## LIST OF TABLES

	<u>Page</u>
Table 1.      Synthesis Conditions and Surface Areas for NO <sub>x</sub> Decomposition Catalysts Prepared During Phase I	6
Table 2.      Catalysts Initially Evaluated During Phase I. GSV = 3200 h <sup>-1</sup>	10
Table 3.      Oxygen Dependence of NO Reduction Activity of (Bi <sub>2</sub> O <sub>3</sub> ) <sub>0.8</sub> (Nb <sub>2</sub> O <sub>5</sub> ) <sub>0.2</sub> . T = 750°C. GHSV = 3200 h <sup>-1</sup>	11
Table 4.      Data Obtained Using Catalyst 2b. T = 500°C.	11
Table 5.      Summary of Activity Data Obtained by Mass Spectrometry for Base-Promoted Catalysts Experimentally Evaluated During Task 2. 1000 ppm NO	15
Table 6.      Average Metal - Oxygen Binding Energies for Base - Promoted Catalysts Studied	16
Table 7.      Summary of Data for Preferred Catalysts Studied During Phase I. All Data with 16% O <sub>2</sub> , 500 ppm NO in the Absence of an Intentionally Introduced Reductant	31

## I. INTRODUCTION

### A. Objective

The objective of this Phase I Small Business Innovation Research (SBIR) project was to evaluate new catalysts for achieving the high rate decomposition of nitrogen oxides under conditions representative of those encountered in the exhausts of gas turbines such as air breathing propulsion systems (jet engines). This subject is of importance to the Air Force in several respects, including the reduction of the chemical signatures of jet propelled aircraft and emissions reduction in stationary sources of  $\text{NO}_x$ .

### B. Program Background

The overall approach employed in this project was directed toward development of catalysts compatible with high operating temperatures, very short (submillisecond) residence times, oxygen-rich (10 - 20 percent) environments, and the presence of potentially poisoning ( $\text{SO}_2$  and  $\text{CO}_2$ ) or destabilizing ( $\text{H}_2\text{O}$ ) species in the exhaust stream. The approach is of specific interest to the Air Force because of the potential reduction in chemical (e.g., IR) signature resulting from  $\text{deNO}_x$  catalysts under development in this program. Work performed has demonstrated catalysts possessing attributes amenable to  $\text{deNO}_x$  activity under net oxidizing reagentless conditions. Catalyst properties of particular interest were anticipated to be metal - oxygen binding energy, basicity, and electronic configuration of the transition-metal ion. A schematic of the overall process and mechanistic features anticipated to be active in this approach are shown in Figure 1. In this case, uptake of nitrogen oxides under net oxidizing conditions is enhanced by the catalyst basicity.

The equilibrium



is shifted to the right under these conditions and so the uptake of  $\text{NO}_x$  is enhanced by the presence of excess oxygen. Because  $\text{NO}_2$  is anticipated to be a much stronger Lewis acid than is  $\text{O}_2$ , competition by  $\text{O}_2$  for adsorption sites is strongly reduced.

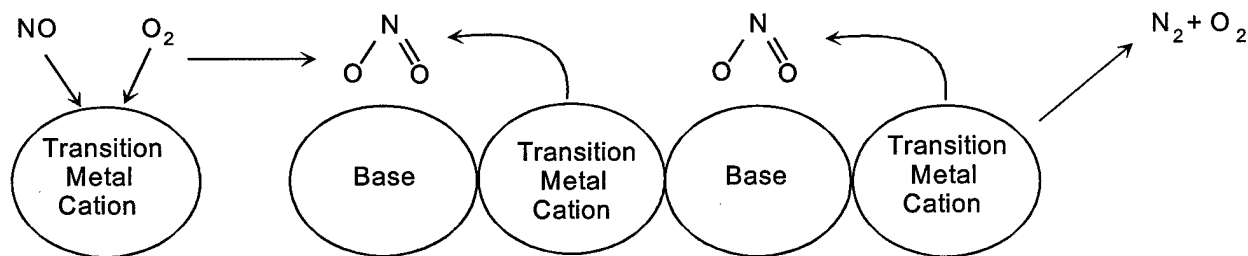


**Figure 1. Schematic of catalyst mechanistic features of approach for promoting  $\text{NO}_x$  decomposition.**

The method used for design and selection of catalysts may be described as "genetic." This approach consisted of first proposing a series of catalysts with potentially favorable properties. These catalysts were initially screened and those demonstrating statistically significant activity towards  $\text{NO}_x$  decomposition selected for modification. Modifications (in terms of basicity, different ratios of transition metal ions, metal - oxygen binding energies) were then incorporated via synthesis of the proposed materials. The experimental performance of these de $\text{NO}_x$  catalysts was determined and further modifications were suggested. The "decision tree" addressed in this screening approach is shown in Figure 2. The effect of this screening procedure was to accumulate favorable variations in catalyst compositions compatible with achieving high activity towards  $\text{NO}_x$  decomposition under net oxidizing conditions.

### C. Scope

This report describes research done under the DoD Small Business Innovation Research (SBIR) program, Contract No. F41624-97-C-0010, "High-Temperature Heterogeneous Redox Catalysis for  $\text{NO}_x$  Abatement." The impetus for the program comes from the need to reduce the chemical signatures of jet propelled aircraft in the Air Force combat inventory. Methods currently available are insufficient for this purpose. Particularly troublesome is the nature of gas turbine exhausts: extremely high (> 15 percent) levels of oxygen, which tend to poison catalysts, are encountered in these sources. Catalytic approaches have, until the present, failed under these conditions. Results presented in the report indicate that this barrier has been overcome and that

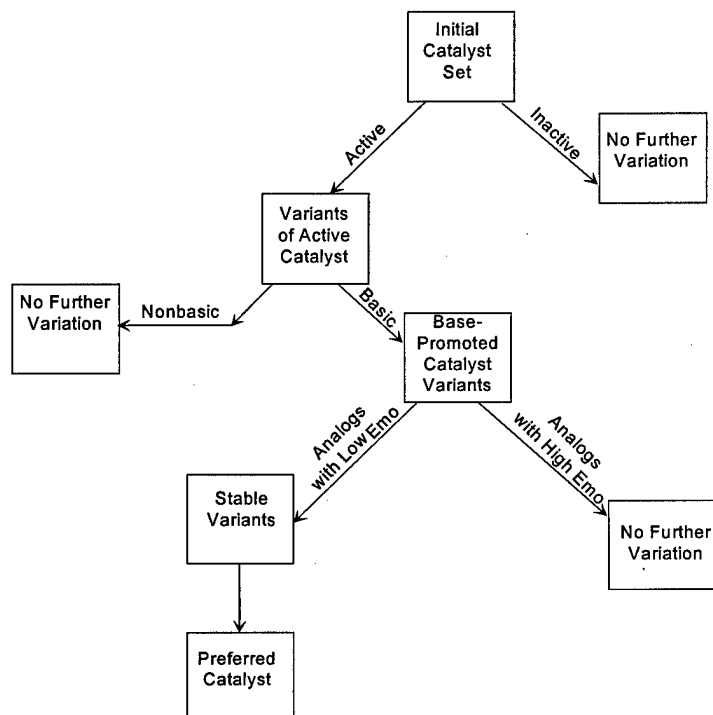


**Figure 2.** Decision tree used during Phase I for selection of preferred  $\text{NO}_x$  decomposition catalysts.

a reagentless catalysis system for deNO<sub>x</sub> of gas streams is now available.

## II. PHASE I TECHNICAL OBJECTIVES

This program addressed the synthesis, characterization, and optimization of heterogeneous catalysts compatible with promoting spontaneous NO<sub>x</sub> decomposition under net oxidizing conditions under anticipated Air Force combustion exhaust manifold conditions. Two catalyst classes were initially proposed to be examined which were based on activities previously determined at Eltron.

Systematic variations of compositions of the proposed materials were performed to effect variation in catalyst metal-oxygen bond strengths, basicity, and NO<sub>x</sub> decomposition activity (oxygen vacancy concentration, facility towards rereduction of active site, etc). Preferred variants of these catalysts, following immobilization into a ceramic honeycomb monolithic structure, were applied towards decomposing NO<sub>x</sub> under net oxidizing conditions.

Effort was directed towards synthesis, characterization and optimization of catalysts for NO<sub>x</sub> decomposition under net oxidizing conditions both present and absent of reducing agent (C<sub>3</sub>H<sub>8</sub>, C<sub>3</sub>H<sub>6</sub>, or CO). Substrates were subsequently selected as supports for preferred NO<sub>x</sub> decomposition catalysts. Initial catalyst compositions were based on those experimentally demonstrating encouraging activity towards NO<sub>x</sub> decomposition under net oxidizing conditions. Following optimization of catalyst composition and subsequent support/substrate selection, resulting honeycomb monoliths were performance tested.

**Specific objectives addressed during this program may be summarized as follows:**

- Synthesize heterogeneous catalysts by either calcining the initial stoichiometric oxides or application of coprecipitation techniques. Catalysts of other compositions were also prepared. This was followed by X-ray diffraction analysis to determine phase purity and crystallographic lattice constants. Surface area analysis was performed by application of the BET (Brunauer - Emmett - Teller) method to determine catalyst surface areas.
- Experimentally determined correlations between rate of catalysis activity of NO<sub>x</sub> decomposition under net oxidizing conditions and correlations with catalyst physical parameters such as i) metal - oxygen bond energy, ii) the crystallographic phase present, iii) catalyst lattice parameters, iv) calculated catalyst electronic considerations such as d-orbital occupancy and calculated Fermi level position, and v) general experimental operating conditions including the concentrations of CO, CO<sub>2</sub>, SO<sub>2</sub>, H<sub>2</sub>O, O<sub>2</sub>, and hydrocarbon (C<sub>3</sub>H<sub>8</sub>, or C<sub>3</sub>H<sub>6</sub>) present with the NO<sub>x</sub> containing feedstream. Selection of preferred catalysts was assisted by a statistical analysis approach.
- For preferred defined catalyst composition, identified correlations between NO<sub>x</sub> - decomposing activity and procedure used for catalyst preparation.
- Experimentally identified preferred honeycomb supports for immobilizing catalysts for subsequent application and performance evaluation. Evaluated activity of supported catalysts.

These initially proposed experimental objectives were modified to reflect the following:

- Catalyst which demonstrated high activity during our initial experimental evaluation towards  $\text{NO}_x$  decomposition were further modified in composition in terms of those features or attributes thought to give rise to activity.
- Most - active variants were further modified in properties (e.g., basicity, metal - oxygen binding energy, transition- metal cations) demonstrated to give rise to activity.
- The most-stable and -active variants of the above were selected to be supported on  $\text{NO}_x$  decomposition powders or monoliths.
- Activity of supported catalysts towards  $\text{NO}_x$  decomposition under net oxidizing conditions was evaluated.

### III. WORK PERFORMED AND RESULTS OBTAINED

The overall objective of work performed was to identify preferred catalyst compositions for promoting the direct decomposition of nitrogen oxides in exhaust streams containing excess oxygen up to 16 volume percent. Exhausts incorporated major constituents found in exhausts from Air Force air breathing propulsion units, internal combustion (diesel) engines, and incinerators. Such catalysts must be compatible with high temperatures as well as feedstream oxygen, water, sulfur dioxide, and carbon dioxide.

Work performed included synthesis and X-ray powder diffraction pattern characterization of catalysts as well as surface area determination. Initial screening of catalysts synthesized was performed, followed by a more- thorough characterization, and synthesis and evaluation of their derivatives.

The Phase I program was performed by completing the following three tasks.

*Task 1 Performance Testing of Redox Catalysts for  $\text{NO}_x$  Decomposition*

*Task 2 Optimization of Catalysts*

*Task 3 Selection and Performance Testing of Supported Catalysts*

Work performed in each of these tasks will now be discussed.

#### *Task 1 Performance Testing of Redox Catalysts for $\text{NO}_x$ Decomposition*

##### **A. Synthesis of Catalysts**

Catalysts prepared during Phase I were synthesized by either 1) a ceramic method (i.e., from the oxides), 2) coprecipitation, or 3) by impregnation of powdered supports. A brief description of each of these procedures performed during Phase I is presented in the following paragraphs.

Preparation of materials by the oxide method was as follows. Constituent metal oxides of

the catalysts were mixed in the appropriate stoichiometric ratios by ball milling in 2-propanol for 24 hours. Following evaporation of alcohol, each mixture was calcined in an alumina crucible in a Lindbergh 1500°C furnace.

Coprecipitation of catalysts was carried out as follows. Stoichiometric ratios of constituent metal ions were prepared in aqueous solutions of metal nitrates. The equivalent concentration of the metal ions was of the order of 0.1M for the limiting (preponderant) ion. A precipitant (1 - 5M  $\text{NH}_4\text{OH}$ ,  $\text{NH}_4(\text{CO}_3)_2$ , or  $\text{K}_2\text{CO}_3$ ) was then added slowly with stirring until an amount of precipitant just exceeding the stoichiometric amount was added. Precipitates were then suction filtered and washed three times with 5 mL of cold deionized water. Suction filtering was continued until the precipitate was cracked. The precipitates were then dried at 110°C, followed by calcination at 400°C for 4 hours.

Supported catalysts were prepared by a slurry technique. In this approach, solutions of metal nitrates were prepared such that their concentrations were sufficient to achieve a desired loading of metal oxide on the support by just saturating the powder with solution. This slurry was then dried and calcined. Catalyst loading was calculated assuming complete uptake by the support.

Following calcination, X-ray powder diffraction patterns for each catalyst was obtained using a Rigaku Miniflex powder diffractometer equipped with a copper source. Table 1 summarizes calcination conditions for catalysts prepared in Phase I. Surface areas of catalysts were determined by the Brunauer - Emmett - Teller (BET) method using an ASAP 2000 surface area analyzer/porosimeter (Micromeritics) with nitrogen as the adsorbate molecule. Initial surface area measurements for some of the materials are also summarized in Table 1.

An interesting observation concerning this data is that coprecipitation techniques employing alkali metals typically gave lower surface areas than catalysts prepared from the oxides or precipitated with  $\text{NH}_4\text{OH}$  or  $(\text{NH}_4)_2\text{CO}_3$ . It is doubtful that this was due to sintering enhancement. Most likely, the alkali-metal oxide formed a low-melting phase which served to fill in pores of the metal oxide matrix. The highest surface areas were obtained from ammonium hydroxide coprecipitation of cerium-oxide-based catalysts.

## B. Catalyst Testing

Catalysts prepared as in the previous subtask were now experimentally evaluated towards  $\text{NO}_x$  decomposition. The catalysts were screened using the apparatus shown in Figure 3. The reactor (Figure 4) was fabricated from quartz tubing of inside diameter 14 mm and packed with 0.25 - 1.0 g of the catalyst held in place with quartz wool plugs. Gases were delivered into the reactor through stainless-steel tubing interfaced to the reactor with stainless-steel fittings. Gas-sampling ports were present in the apparatus to allow gas-chromatographic analysis of inlet and exhaust streams. Inlet and exhaust streams were, at this point, primarily sampled by a Residual Gas Analyzer (RGA) for identification and quantitation of reactants and products. The RGA was based on a Leybold - Inficon quadrupole mass spectrometer with a 200-amu mass range.

The analysis space was pumped using a Leybold Vacuum Products TMP/NT-150 turbo molecular pump backed with a Leybold Vacuum Products Trivac A dual-stage rotary-vane pump. Gas samples were introduced into the analysis space with a manually controlled molecular leak valve. The leak valve was adjusted to a total pressure that was, at minimum,  $5 \times 10^{-5}$  torr. Sampling consisted of opening the reactor exhaust to the mass spectrometer and diverting the

**Table 1.**  
**Synthesis Conditions and Surface Areas for NO<sub>x</sub>**  
**Decomposition Catalysts Prepared During Phase I**

#	Material	Preparation Method	Calcination		BET Surface Area (m <sup>2</sup> /g)
			Temp (°C)	Time (hr)	
1	Catalyst 1	From Oxides	900	2	1.1538 +/- 0.0383
2	Catalyst 2	From Oxides	700	2	5.2947 +/- 0.0579
3	(U <sub>3</sub> O <sub>8</sub> ) <sub>0.8</sub> (CuO) <sub>0.2</sub>	From Oxides	900	2	3.0847 +/- 0.0192
4	Catalyst 4	From Oxides	900	2	5.1717 +/- 0.0415
5	Catalyst 5	From Oxides	900	2	6.2309 +/- 0.0591
6	Zr <sub>0.6</sub> Ce <sub>0.1</sub> Co <sub>0.15</sub> Cu <sub>0.15</sub> O <sub>1.75</sub>	From Oxides	900	2	5.8879 +/- 0.0236
7	Zr <sub>0.6</sub> Ce <sub>0.1</sub> Cu <sub>0.3</sub> O <sub>1.7</sub>	From Oxides	900	2	2.1941 +/- 0.0571
9	(U <sub>3</sub> O <sub>8</sub> ) <sub>0.8</sub> (CuO) <sub>0.1</sub> (Co <sub>3</sub> O <sub>4</sub> ) <sub>0.1</sub>	From Oxides	900	2	0.7506 +/- 0.0384
10	Bi(WO <sub>4</sub> ) <sub>3</sub>	From Oxides	750	2	3.9551 +/- 0.0090
11	Cu <sub>0.2</sub> Sr <sub>0.8</sub> Al <sub>12</sub> O <sub>19</sub>	From Oxides	1000	2	1.0644 +/- 0.0379
12	SrAl <sub>12</sub> O <sub>19</sub>	From Oxides	1200	2	0.9144 +/- 0.0208
13	Cu <sub>0.5</sub> Co <sub>0.5</sub> Al <sub>2</sub> O <sub>4</sub>	From Oxides	900	2	1.3358 +/- 0.0174
14	Co <sub>0.1</sub> Cu <sub>0.1</sub> Sr <sub>0.8</sub> Al <sub>12</sub> O <sub>19</sub>	From Oxides	900	2	1.3577 +/- 0.0166
15	Catalyst 15	From Oxides	900	2	2.1465 +/- 0.0153
16	Cu <sub>0.5</sub> Co <sub>0.5</sub> Ga <sub>2</sub> O <sub>4</sub>	From Oxides	900	2	
17	Nd <sub>2</sub> CuO <sub>4</sub>	From Oxides	900	2	
18	Catalyst 18	From Oxides	900	2	0.5703 +/- 0.0295
19	Ce <sub>0.9</sub> Zn <sub>0.1</sub> O <sub>1.9</sub>	From Oxides	900	2	
20	ZnCe <sub>0.8</sub> Fe <sub>0.2</sub> O <sub>2.9</sub>	From Oxides	900	2	
21	ZnCeO <sub>3</sub>	From Oxides	900	2	
22	Sr <sub>2</sub> Bi <sub>2</sub> Cu <sub>2</sub> O <sub>7</sub>	From Oxides	800	2	1.2594 +/- 0.0177
23	LaBa <sub>2</sub> Cu <sub>3</sub> O <sub>7</sub>	From Oxides	900	2	
24	Sr <sub>2</sub> Gd <sub>2</sub> O <sub>3</sub>	From Oxides	900	2	
25	Sr <sub>2</sub> La <sub>2</sub> O <sub>5</sub>	From Oxides	900	2	
26	ZnFe <sub>2</sub> O <sub>4</sub>	From Oxides	900	2	
27	CuCoO <sub>4</sub>	From Oxides	900	2	0.8871 +/- 0.260
29	CuFe <sub>2</sub> O <sub>4</sub>	From Oxides	900	2	
30	Catalyst 30	PPT From Nitrates	400	2	55.5442 +/- 0.2484
31	Catalyst 31	Precipitated	400	2	4.3703 +/- 0.0163
32	Catalyst 32	Coprecipitated	400	2	4.0814 +/- 0.0337
33A	Catalyst 33A	From Nitrates	800	2	101.3473 +/- 0.3615
33B	Catalyst 33B	From Nitrates	400	2	143.5918 +/- 0.8243
34	Zr <sub>0.7</sub> Ni <sub>0.3</sub> O <sub>1.3</sub>	From Nitrate Gel	600	1	16.4797 +/- 0.1352
35	Catalyst 35	From Oxides	900	2	
36	Catalyst 36	From Oxides	900	2	1.2299 +/- 0.0216
37	LaSrCuAlO <sub>5</sub>	From Oxides	1000	2	
38	LaSrCuGaO <sub>5</sub>	From Oxides	1000	12	
39	Catalyst 39	From Oxides	900	2	
40	Sr <sub>1.6</sub> La <sub>0.4</sub> Ga <sub>0.6</sub> Fe <sub>1.2</sub> Co <sub>0.2</sub> O <sub>5</sub>	From Oxides	1000	12	1.7250 +/- 0.0243
41	Catalyst 41	From Oxides	900	2	1.7565 +/- 0.0150
42	Catalyst 42	From Oxides	900	2	

**Table 1. (Continued)**  
**Synthesis Conditions and Surface Areas for NO<sub>x</sub>**  
**Decomposition Catalysts Prepared During Phase I**

#	Material	Preparation Method	Calcination		BET Surface Area (m <sup>2</sup> /g)
			Temp (°C)	Time (hr)	
43	Bi <sub>0.6</sub> W <sub>3</sub> O <sub>12</sub>	From Oxides	750	2	1.0732 +/- 0.0035
44	Pr <sub>0.6</sub> W <sub>3</sub> O <sub>12</sub>	From Oxides	900	2	
45	Bi <sub>2</sub> VO <sub>5.5</sub>	From Oxides	750	2	1.0440 +/- 0.0458
46	CuWO <sub>4</sub>	As Received			15.2147 +/- n0.0495
47	(2.6	From Oxides	900	2	
48	(Bi <sub>2</sub> O <sub>3</sub> ) <sub>0.8</sub> (WO <sub>3</sub> ) <sub>0.2</sub>	From Oxides	750	2	0.2023 +/- 0.0185
49	(Bi <sub>2</sub> O <sub>3</sub> ) <sub>0.8</sub> (Nb <sub>2</sub> O <sub>5</sub> ) <sub>0.2</sub>	From Oxides	750	2	0.8174 +/- 0.0078
50	Catalyst 50	From Oxides	900	2	1.6015 +/- 0.0241
51	BiWO <sub>4.5</sub>	From Oxides	750	2	0.5158 +/- 0.0094
52	Bi <sub>2</sub> (WO <sub>4</sub> ) <sub>3</sub>	From Oxides	750	2	1.0465 +/- 0.0177
53	(Bi <sub>2</sub> O <sub>3</sub> ) <sub>0.6</sub> (Nb <sub>2</sub> O <sub>5</sub> ) <sub>0.4</sub>	From Oxides	750	2	
54	(Bi <sub>2</sub> O <sub>3</sub> ) <sub>0.5</sub> (Nb <sub>2</sub> O <sub>5</sub> ) <sub>0.5</sub>	From Oxides	750	2	
55	(Bi <sub>2</sub> O <sub>3</sub> ) <sub>0.4</sub> (Nb <sub>2</sub> O <sub>5</sub> ) <sub>0.6</sub>	From Oxides	750	2	1.7007 +/- 0.0324
56	(Bi <sub>2</sub> O <sub>3</sub> ) <sub>0.8</sub> (CeO <sub>2</sub> ) <sub>0.2</sub>	From Oxides	750	2	
57	(Bi <sub>2</sub> O <sub>3</sub> ) <sub>0.8</sub> (ZrO <sub>2</sub> ) <sub>0.2</sub>	From Oxides	750	2	
58	(Bi <sub>2</sub> O <sub>3</sub> ) <sub>0.8</sub> (Y <sub>2</sub> O <sub>3</sub> ) <sub>0.2</sub>	From Oxides	750	2	
59	(Bi <sub>2</sub> O <sub>3</sub> ) <sub>0.8</sub> (La <sub>2</sub> O <sub>3</sub> ) <sub>0.2</sub>	From Oxides	750	2	
60	(Bi <sub>2</sub> O <sub>3</sub> ) <sub>0.8</sub> (Gd <sub>2</sub> O <sub>3</sub> ) <sub>0.2</sub>	From Oxides	750	2	
63	(Bi <sub>2</sub> O <sub>3</sub> ) <sub>0.6</sub> (Nb <sub>2</sub> O <sub>5</sub> ) <sub>0.2</sub> (Co <sub>3</sub> O <sub>4</sub> ) <sub>0.2</sub>	From Oxides	750	2	
64	(Bi <sub>2</sub> O <sub>3</sub> ) <sub>0.8</sub> (Ta <sub>2</sub> O <sub>5</sub> ) <sub>0.2</sub>	From Oxides	750	2	
65	Bi(MoO <sub>4</sub> ) <sub>3</sub>	From Oxides	750	2	
66	(Bi <sub>2</sub> O <sub>3</sub> ) <sub>0.8</sub> (V <sub>2</sub> O <sub>5</sub> ) <sub>0.2</sub>	From Oxides	750	2	
67	(Bi <sub>2</sub> O <sub>3</sub> ) <sub>0.6</sub> (WO <sub>3</sub> ) <sub>0.4</sub>	From Oxides	750	2	0.2625 +/- 0.0189
68	(Bi <sub>2</sub> O <sub>3</sub> ) <sub>0.5</sub> (WO <sub>3</sub> ) <sub>0.5</sub>	From Oxides	750	2	
69	(Bi <sub>2</sub> O <sub>3</sub> ) <sub>0.4</sub> (WO <sub>3</sub> ) <sub>0.6</sub>	From Oxides	750	2	1.6563 +/- 0.0242
70	Catalyst 70	PPT From Nitrates	400	2	0.6621 +/- 0.0453
71	Zr <sub>0.6</sub> V <sub>0.4</sub> O <sub>2</sub>	PPT From Nitrates	900	1	0.6773 +/- 0.0300
72	Zr <sub>0.6</sub> Fe <sub>0.4</sub> O <sub>2</sub>	PPT From Nitrates	900	1	2.9994 +/- 0.0128
73	Zr <sub>0.6</sub> Cu <sub>0.4</sub> O <sub>2</sub>	PPT From Nitrates	900	1	3.4402 +/- 0.0294
74	BiV <sub>2</sub> O <sub>6.5</sub>	From Oxides	750	2	0.8865 +/- 0.0748
75	BiNb <sub>2</sub> O <sub>6.5</sub>	From Oxides	750	2	2.0699 +/- 0.0191
76	Bi(MoO <sub>4</sub> ) <sub>3</sub>	From Oxides	600	2	0.8007 +/- 0.0208
77	CaWO <sub>4</sub>	As Received			1.1641 +/- 0.0211
78	Catalyst 78	From Oxides	1200	8	
79	Catalyst 79	From Oxides	1000	8	1.7582 +/- 0.0167
80	Na <sub>2</sub> WO <sub>4</sub> •2H <sub>2</sub> O	As Received			2.4134 +/- 0.0110
81	Catalyst 81	From Oxides	750	2	0.9189 +/- 0.0140
82	Catalyst 82	From Oxides	750	2	1.2242 +/- 0.0337
83	Catalyst 83	From Oxides	750	2	0.8225 +/- 0.0089
84	Catalyst 84	From Oxides	900	2	2.4166 +/- 0.0342

**Table 1. (Concluded)**  
**Synthesis Conditions and Surface Areas for NO<sub>x</sub>**  
**Decomposition Catalysts Prepared During Phase I**

#	Material	Preparation Method	Calcination		BET Surface Area (m <sup>2</sup> /g)
			Temp (°C)	Time (hr)	
93	Catalyst 93	PPT From Nitrates	400	2	2.5463 +/-0.0343
94	Catalyst 94	From Oxides	750	2	
95	Catalyst 95	From Oxides	750	2	
96	Catalyst 96	From Oxides	750	2	
97	Catalyst 97	From Oxides	750	2	
98	Catalyst 98	From Oxides	850	2	
99	Catalyst 99	From Oxides	850	2	
100	Catalyst 100	From Oxides	850	2	
101	Catalyst 101	From Oxides	850	2	
102	Catalyst 102	From Oxides	1000	4	0.5966 +/-0.0152
103	Catalyst 103	From Oxides	1000	4	
104	Catalyst 104	From Oxides	750	2	0.5771 +/- 0.0183
105	Catalyst 105	From Oxides	1000	8	0.6312 +/- 0.0334
106	Catalyst 106	From Oxides	1000	8	1.2294 +/- 0.0377
107	Catalyst 107	From Oxides	1000	8	
108	Catalyst 108	From Oxides	1000	8	1.4357 +/- 0.0311
109	Catalyst 109	From Oxides	1000	8	
110	Catalyst 110	From Oxides	1000	8	
111	Catalyst 111	From Oxides	850	2	
112	Catalyst 112	From Oxides	850	2	
113	Catalyst 113	From Oxides	1000	8	
114	Catalyst 114	From Oxides	850	2	

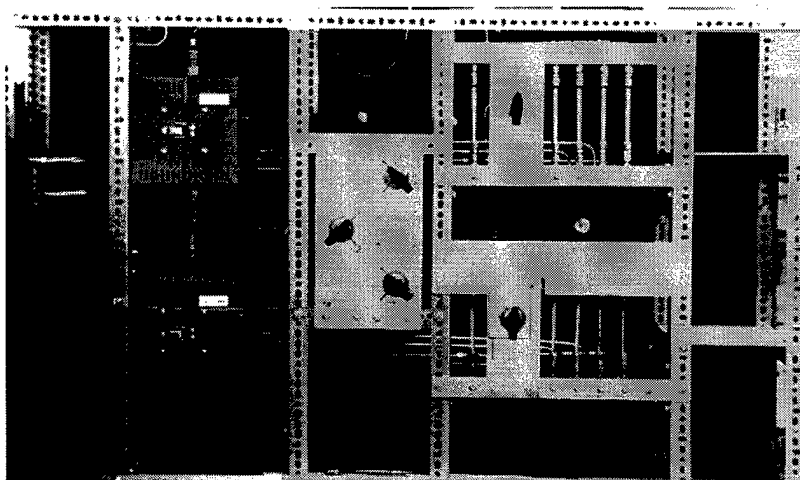


**Figure 3. Photograph of Catalyst Test Stand Used to Characterize the Performance of DeNO<sub>x</sub> Catalysts.**

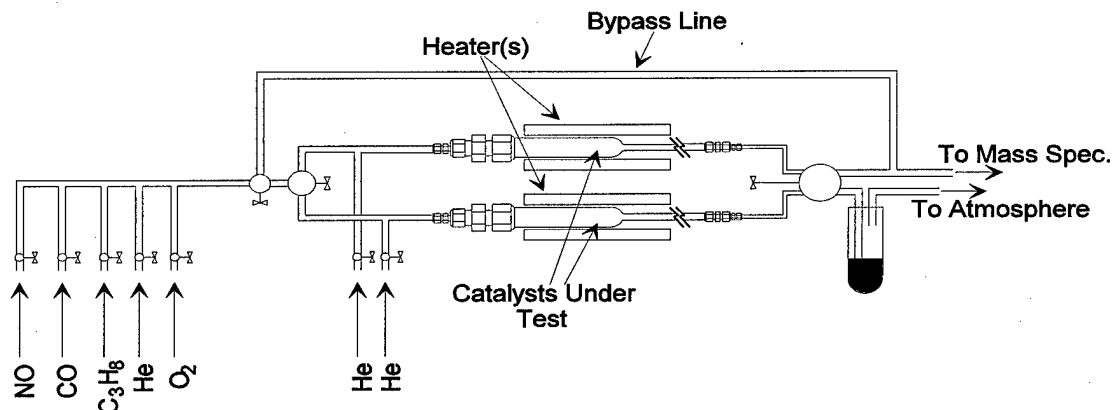


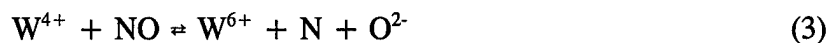
**Figure 4. Schematic of dual reactor system incorporating a quadrupole mass spectrometer for study of high temperature NO<sub>x</sub> decomposition under net oxidizing conditions.**

stream through a bypass channel to the mass spectrometer to obtain the baseline reactor inlet concentration. The utility of this approach was later corroborated by use of electrochemical NO<sub>x</sub> sensors. Data for catalysts initially screened for deNO<sub>x</sub> are shown in Table 2. Three pieces of information can be immediately deduced from Table 2: 1) an absence of correlation between surface area and activity, 2) the high activity of bismuth tungstates and niobates relative to other materials, and 3) the large improvement in the catalytic activity of catalyst 2b obtained by coprecipitation versus synthesis from the oxides (catalyst 2a). The first point clearly indicates that composition plays a major role over and above catalyst surface area. This is an extremely important consideration in selectionist or genetic approaches, as employed during this Phase I: even given the necessarily constrained compositions of materials, the distribution of features among compositions should be random if a selectionist approach is to work properly.

The data for percent conversion of NO by bismuth tungstate at 750°C and at a space velocity of 3200h<sup>-1</sup> is shown as a function of the W/Bi ratio in Figure 5. This plot shows a maximum in activity at a W/Bi ratio of 3. The reasons for this are not clear, but apparently, may involve competition between intercationic electron transfer and other issues, e.g. metal - oxygen binding energy. For example, the equilibrium



would allow for the decomposition of NO via adsorption onto the surface and a two-electron transfer from W<sup>4+</sup> to NO:



Unless a reagent is present, however, regeneration of Bi<sup>3+</sup> and W<sup>4+</sup> is not possible. This category of materials did not appear to be oxygen tolerant, and so was not pursued further.

An analog of the tungstate material was obtained by solid-state reaction of Bi<sub>2</sub>O<sub>3</sub> and Nb<sub>2</sub>O<sub>5</sub>. Unlike the tungstates, however, some oxygen tolerance was observed. Again, explanation

**Table 2.**  
**Catalysts Initially Evaluated During Phase I. GSV = 3200 h<sup>-1</sup>**

No.	Material	% NO Removed	BET Surface Area (m <sup>2</sup> /g)
1	Catalyst 1	6	1.15
2a	Catalyst 2a	0	5.29
2b	Catalyst 2b	100	0.66
5	Catalyst 5	4	6.23
6	Zr <sub>0.6</sub> Ce <sub>0.1</sub> Co <sub>0.15</sub> Cu <sub>0.15</sub> O <sub>2</sub>	2	5.89
9	(U <sub>3</sub> O <sub>8</sub> ) <sub>0.8</sub> (CuO) <sub>0.1</sub> (CoO <sub>x</sub> ) <sub>0.1</sub>	0	0.75
10	Bi(WO <sub>4</sub> ) <sub>3</sub>	33	3.96
11	Cu <sub>0.2</sub> Sr <sub>0.8</sub> Al <sub>12</sub> O <sub>19</sub>	0	1.06
13	Cu <sub>0.5</sub> Co <sub>0.5</sub> Al <sub>2</sub> O <sub>4</sub>	0	1.34
18	Catalyst 18	2	0.57
22	Sr <sub>2</sub> Bi <sub>2</sub> Cu <sub>2</sub> O <sub>7</sub>	1	1.26
27	CuCo <sub>2</sub> O <sub>4</sub>	4	0.89
33A	Catalyst 33A	1	101.3
36	Catalyst 36	0	1.23
40	Sr <sub>1.6</sub> La <sub>0.4</sub> Ga <sub>0.6</sub> Fe <sub>1.2</sub> Co <sub>0.2</sub> O <sub>5</sub>	0	1.73
41	Catalyst 41	4	1.76
43	Bi <sub>0.6</sub> W <sub>3</sub> O <sub>12</sub>	6	1.07
45	Bi <sub>2</sub> VO <sub>5.5</sub>	0	1.04
46	CuWO <sub>4</sub>	0	15.2
48	(Bi <sub>2</sub> O <sub>3</sub> ) <sub>0.8</sub> (WO <sub>3</sub> ) <sub>0.2</sub>	0	0.20
49	(Bi <sub>2</sub> O <sub>3</sub> ) <sub>0.8</sub> (Nb <sub>2</sub> O <sub>5</sub> ) <sub>0.2</sub>	22	0.82
50	Catalyst 50	0	1.60
51	BiWO <sub>4.5</sub>	16	0.52
52	Bi <sub>2</sub> (WO <sub>4</sub> ) <sub>3</sub>	12	1.05
55	(Bi <sub>2</sub> O <sub>3</sub> ) <sub>0.4</sub> (Nb <sub>2</sub> O <sub>5</sub> ) <sub>0.6</sub>	0	1.70

is difficult, although comparison of metal - oxygen bond energies for WO<sub>3</sub> and Nb<sub>2</sub>O<sub>5</sub> shows that the latter has an E<sub>MO</sub> of 81 kcal/mole versus 97 for the former. The third piece of information derived from Table 2 is the promotional effect of added bases on catalytic deNO<sub>x</sub>. This effect will be elaborated on in the following paragraphs.

In the case of Catalyst 2b, 100 percent removal of NO was obtained at space velocities of between 3200 and 44000h<sup>-1</sup> in the presence of 16 percent O<sub>2</sub>. Data for this material are presented in Table 4. The drastic difference in the activity relative to that of materials (Table 2) that were prepared from the oxides is not accompanied by great structural differences. The X-ray diffraction patterns of these materials clearly reflect this assertion and are compared in Figure 6.

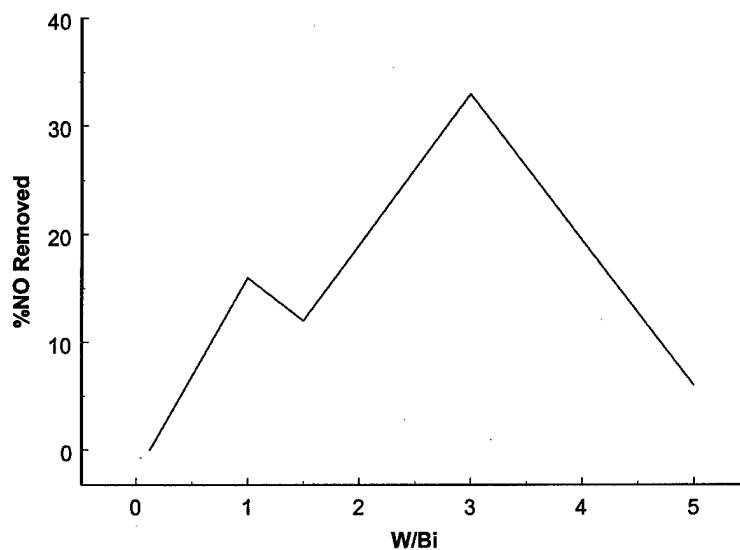


**Figure 5.** Plot of %NO removed at 750°C and 3200 h<sup>-1</sup> over bismuth tungstate catalysts in Table 3.

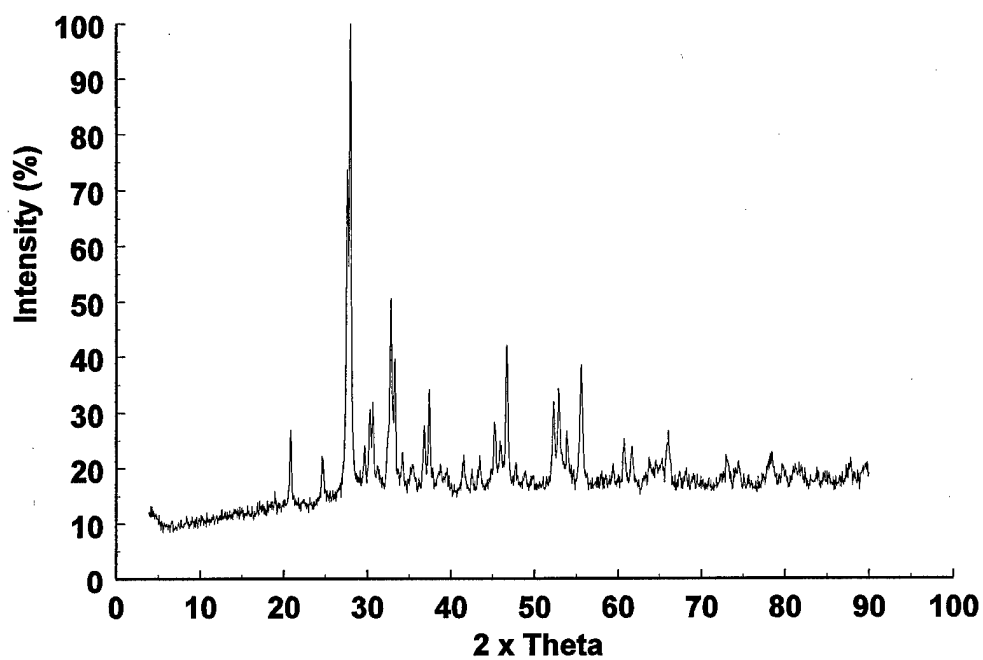
**Table 3.**  
Oxygen Dependence of NO Reduction Activity  
of (Bi<sub>2</sub>O<sub>3</sub>)<sub>0.8</sub>(Nb<sub>2</sub>O<sub>5</sub>)<sub>0.2</sub>. T = 750°C. GHSV = 3200 h<sup>-1</sup>

Vol. % O <sub>2</sub>	%NO Removed
0	22
2	21
8	14

**Table 4.**  
Data Obtained Using Catalyst 2b.  
T = 500°C.

Vol. % O <sub>2</sub>	Space Velocity	NO Conc. (ppm)	%NO Removed
0	3200	1000	100
16	3200	1000	100
16	44000	500	100

A)



B)

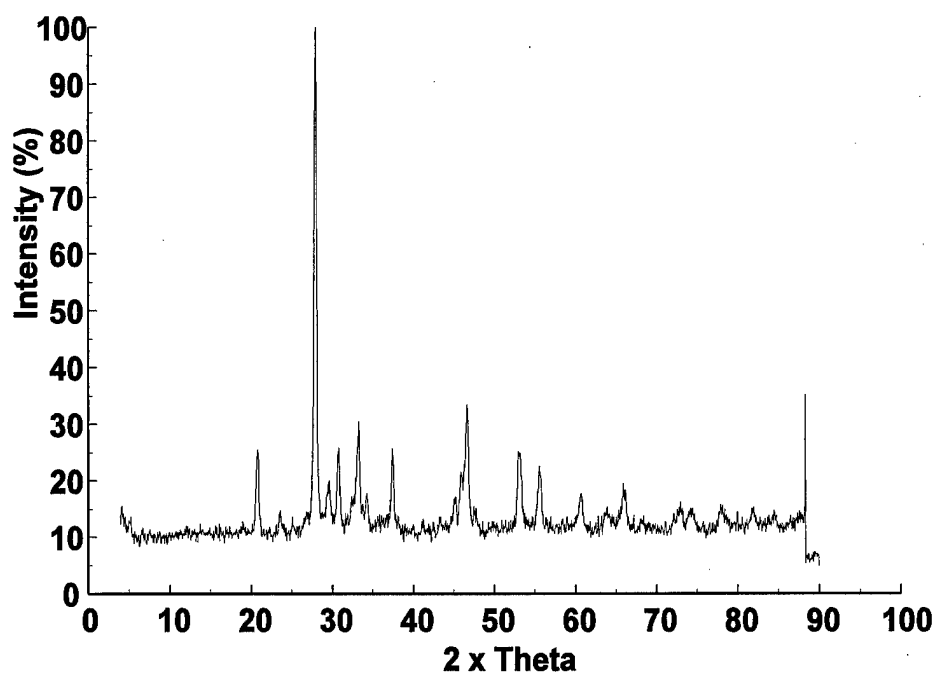


**Figure 6.** X-Ray diffraction pattern of Catalysts 2a and 2b synthesized respectively A) from oxides and B) by coprecipitation.

The diffraction patterns for the two materials are similar, particularly at low angles where peaks such as those at  $\approx 20$  and  $25^\circ$  appear, indicating structural similarity. However, the splitting of a number of peaks suggests different symmetry or structural features in the two materials, perhaps arising, *e.g.*, from a tetragonal versus cubic unit cell. It is not probable, however, that these structural differences are the source of activity differences. Rather, the higher activity obtained with coprecipitated catalysts suggests base promoted decomposition of NO, presumably via acid-base interaction between the catalyst surface and (B:) NO<sub>x</sub>:



The presence of the strongly basic potassium species was detected with energy dispersive X-ray spectroscopy (EDX). The greater acidity of NO<sub>2</sub> versus that of NO suggests that conditions favoring oxidation of NO will lead to a higher surface coverage of nitrogen oxide species. Consequently, deNO<sub>x</sub> rate should *increase* with increased exhaust stream oxygen content. The base component of the catalyst may serve as an adsorption site for reactant but may also serve as a decomposition site. This is confirmed by the work reported by Lyon<sup>1</sup> and by recent work done by Lunsford, et al.,<sup>2</sup> which showed that MgO-supported BaO itself possessed deNO<sub>x</sub> activity. Additionally, Tabata<sup>3</sup> showed that the double perovskite material Ba<sub>2</sub>YCu<sub>3</sub>O<sub>7.8</sub> possessed reagentless activity, with a maximum at about 330°C. Maximum activity was observed with a feedstream oxygen content of 8 percent. It may then be that transition-metal components serve to oxidize NO, resulting in greater uptake of this oxidized form and greater overall activity.

Activity for Catalyst 2b was observed at a space velocity of up to 783,000 h<sup>-1</sup>. However, as can be seen from Figure 7, the activity was transient, occurring for only a few minutes until no measurable activity was evident. Additionally, primarily N<sub>2</sub>O (65-80%), rather than N<sub>2</sub> and O<sub>2</sub> was produced. Both of these issues were resolved later in the program using different catalyst compositions possessing similar functionalities. This was the emphasis of catalysts evaluated during Task 2. Important (influential) features of catalysts were identified. These included basicity and metal-oxygen binding energy.

## Task 2 Optimization of Catalysts

In this task, the results of initial experiments performed in Task 1 were used to define the direction to be taken in the present task. In particular, Task 1 data revealed the importance of basicity in determining catalyst activity towards promoting NO<sub>x</sub> decomposition. Several catalysts observed to have exceptional activity, when synthesized by coprecipitation from media containing basic cations, demonstrated virtually none absent the base. Consequently, it was essentially unnecessary to apply statistical techniques in determining the most-influential catalyst attributes in this case.

In this task we investigated the influence of base and transition metal on various catalyst properties. A number of experiments were performed in which the nature of the base and the transition metal dopant and concentration were varied, but where the synthetic approach was the same in all cases. The data are summarized in Table 5. The influence of base concentration is clearly evident from this Table. It can be seen by comparison of Catalysts 81 and 96 with Catalysts 84 and 98, that a very significant difference was obtained between the cases where the

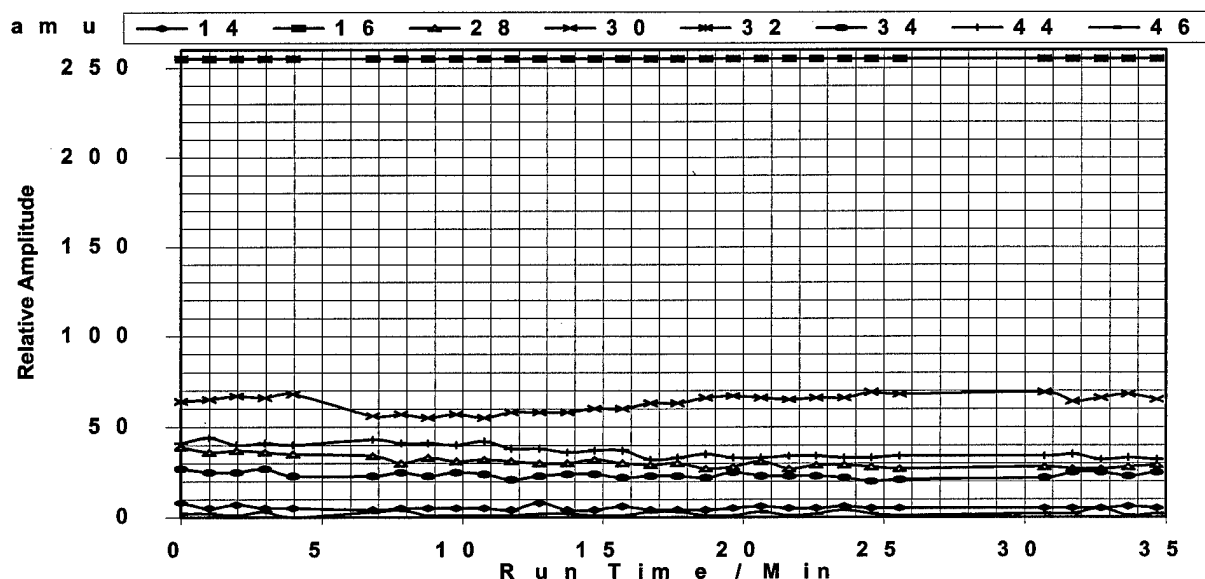


**Figure 7.** Partial pressure data determined by mass spectroscopy for removal of nitrogen oxide (500ppm) from a stream 16% in  $O_2$  over Catalyst 2b. T-500°C.

base cation stoichiometric subscript was varied, with the higher value of the subscript favoring higher activity towards  $NO_x$  decomposition. In the presence of 16 percent  $O_2$ , Catalyst 96, with a base stoichiometric subscript of 0.67 showed, at a space velocity of  $3200h^{-1}$  and 500°C, 100 percent removal of 1000 ppm NO while Catalyst 81, with a base subscript of 0.20, showed only 7 percent removal under the same conditions. It is true that temperatures were 500 and 750°C, respectively, but, as will be shown later, appreciable activity was attainable over other catalysts at much higher space velocities. Similarly, much higher activity was obtained with Catalyst 98, with a base subscript of 0.33, than with Catalyst 84, which possessed a base subscript value of 0.20.

The nature of the basic dopant was found to strongly influence catalyst activities. In particular, the more- weakly basic species Na was found to give appreciably less activity than K in the same material and under the same conditions. However, a very interesting observation concerning the material Catalyst 102 was that conversion of NO was essentially complete under conditions absent of introduced oxygen. The need for the presence of oxygen in the alkali-metal-doped materials apparently arises from the role of oxygen in generating a more-reactive intermediate as in equation 1 (page 1) to participate in the surface process shown in Figure 1 (page 1). It may be that initially surface bound oxygen plays the same role in the case of Catalyst 102 as in the alkali-metal-doped materials.

The effect of varying transition- metal dopants on catalytic activity is shown by comparison of the result for Catalyst 100 with that for Catalyst 98. The latter material gave 100 percent conversion versus only 4 percent for the former. This effect may be rationalized in terms of the lower metal - oxygen bond energy associated with the transition-metal cations in the latter versus that in the former. The calculated M - O bond energies in the two materials above are 83.8 and 67.6kcal/mole, respectively (Table 6). Consequently, as anticipated, the first material was less

**Table 5.**  
**Summary of Activity Data Obtained by Mass Spectrometry for**  
**Base-Promoted Catalysts Experimentally Evaluated During Task 2. 1000 ppm NO**

Material	GHSV (h <sup>-1</sup> )	T (°C)	% O <sub>2</sub>	% NO Decomposed	Product Distribution
Catalyst 79	3200	1000	0 16	0 0	- -
Catalyst 81	3200	750	0 16	0 7	- *
Catalyst 84	3200	900	0 16	0 2	*
Catalyst 96	3200	600	0 16	0 100	- 18% N <sub>2</sub> , 82% N <sub>2</sub> O
	9600	600	0 16	0 100	- 21% N <sub>2</sub> , 79% N <sub>2</sub> O
Catalyst 97	3200	600	0 16	0 61	18% N <sub>2</sub> , 82% N <sub>2</sub> O
Catalyst 98	3200	500	0 16	17 100	29% N <sub>2</sub> , 71% N <sub>2</sub> O 0% N <sub>2</sub> , 100% N <sub>2</sub> O
Catalyst 100	3200	500	0 16	0 4	- *
Catalyst 101	3200	500	0 16	0 6	100% N <sub>2</sub> O
Catalyst 102	3200	500	0 16	95 98	* *
Catalyst 103	3200	500	0 16	44 0	78% N <sub>2</sub> , 22% N <sub>2</sub> O -
Catalyst 104	2810	500	0 16	0 62.5	- *
Catalyst 105	50,000	500	0 16	- 44	- *
Catalyst 106	50,000	500	0 16	- 50	- *
Catalyst 107	50,000	500	0 16	- 20	- *
Catalyst 108	50,000	500	0 16	- 13	- *

\* Interference from desorbing or entrained CO<sub>2</sub> which produced mass 28 and mass 44 peaks, made quantification of N<sub>2</sub> and N<sub>2</sub>O difficult.

active in the presence of oxygen than the second. The presence of more than one transition-metal cation was found to enhance overall activity. For example, it was found later on that 63 percent conversion at 500°C was attainable at a space velocity of 50,000 h<sup>-1</sup> over Catalyst 102 versus only 13% and 20% for the analogs Catalyst 107 and Catalyst 108, respectively, which contained only one of the transition-metal ions.

Results presented in Table 5 pointed to a number of viable potential candidates for further evaluation. It was found, for example, that the material designated as Catalyst 103 demonstrated much higher selectivity to N<sub>2</sub> than did materials doped with alkali metals or coprecipitated from alkali-metal-containing media. Consequently, the particular materials Catalyst 102, Catalyst 105, Catalyst 104, and Catalyst 93 were selected. It should be pointed out that **all of these catalysts demonstrated direct decomposition activity, i.e., products of NO reaction were those anticipated of reduction and not oxidation.** Data for each of these materials will now be presented in order. However, at this stage, the analysis approach included gas-chromatographic detection of N<sub>2</sub>, O<sub>2</sub>, NO, N<sub>2</sub>O, CO<sub>2</sub>, and CO and electrochemical detection of NO and NO<sub>2</sub>. The electrochemical approach was far more sensitive to both of these species than mass spectroscopy. Gas- chromatographic detection of both NO and NO<sub>2</sub> in the presence of O<sub>2</sub> was found to be difficult. Consequently, the use of electrochemical methods was strongly indicated. The experimental setup and protocol for these two approaches will be described in the following paragraphs.

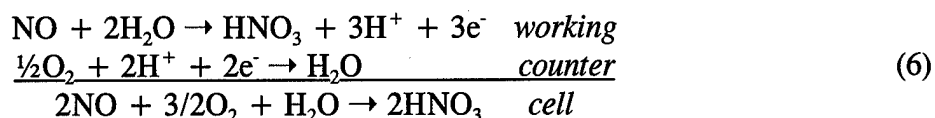
**Table 6.**  
**Average Metal - Oxygen Binding Energies for Base - Promoted Catalysts Studied**

Material	Structure	E <sub>MO</sub> (kcal/mole)
Catalyst 79	Perov./Brownmillerite	62.5
Catalyst 81	Ilmenite	47.6
Catalyst 84	Fluorite	72.7
Catalyst 96	Ilmenite	45.9
Catalyst 97	Ilmenite	46.0
Catalyst 98	Fluorite	67.6
Catalyst 100	Fluorite	83.8
Catalyst 101	Fluorite	84.9
Catalyst 102	Brownmillerite	73.8
Catalyst 103	Fluorite	70.8
Catalyst 104	Brownmillerite	48.3
Catalyst 105	Brownmillerite	75.3
Catalyst 106	Brownmillerite	73.6
Catalyst 107	Brownmillerite	69.1
Catalyst 108	Brownmillerite	71.5

## A. Analysis

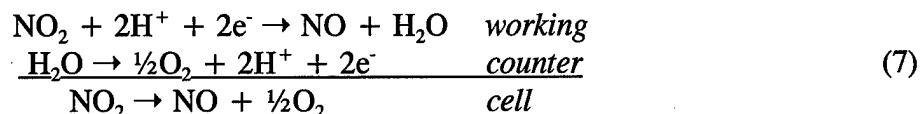
Both NO and NO<sub>2</sub> were measured electrochemically using commercially obtained three-electrode sensors (City Technology, distributed by McNeill International). The sensors were operated in parallel using He as a carrier gas. The He flow was adjusted by a needle valve to approximately 10 mL/min. Samples were introduced with a syringe through injection ports located in the gas stream immediately before each sensor. The gas flow lines through the sensors were made of polytetrafluoroethylene to reduce surface adsorption of NO<sub>2</sub>.

**NO Sensor.** The NO sensor had a nominal measurement range between 0 and 1000 ppm with a resolution of 1 ppm. The sensor was operated under a biased voltage of +300 mV. Detection of NO was achieved potentiometrically from the oxidation of NO at the working electrode. The electrochemical reactions responsible for detection of NO are as follows:



The NO sensor was highly selective; however SO<sub>2</sub>, NO<sub>2</sub> and HCl can produce interferences. An inboard SO<sub>2</sub> filter was included to eliminate interference from SO<sub>2</sub>. Interference from NO<sub>2</sub> and HCl was less severe, accounting for less than 10% and 5% of the NO sensitivity, respectively. The response of the sensor is temperature dependent, but remains consistent within 5% over a temperature range of 10 to 40°C. Sensitivity to pressure changes is eliminated by operating under a continuous carrier gas flow.

**NO<sub>2</sub> Sensor.** The NO<sub>2</sub> sensor had a nominal measurement range between 0 and 1000 ppm with a resolution of 0.5 ppm. A bias potential was not required for operation. Detection of NO<sub>2</sub> was achieved potentiometrically from the reduction of NO<sub>2</sub> at the working electrode. The electrochemical reactions responsible for detection of NO<sub>2</sub> were as follows:



Potentially, the interfering gases and their corresponding percentages of the NO<sub>2</sub> sensitivity were CO (<1%), H<sub>2</sub>S (~-25%), SO<sub>2</sub> (~-3%), NO (<1%), H<sub>2</sub> (<-1%) and HCl (<-1%), where negative values indicate a suppression of the signal. The temperature sensitivity of the NO<sub>2</sub> sensor is approximately the same as the NO sensor.

**GC Analysis.** Effluents directly from the reactor system were analyzed on-line by a gas chromatograph (GC). Data collection was via a serial interface to computer interfaced to an analog-to-digital converter (ADC). The GC was a Hewlett - Packard 5890 Series II with a thermal-conductivity detector. A stainless steel, 35' x 1/8" column was used with Hayesep DB, 100/120-mesh support material. Helium was used as the carrier gas, at a flow rate of 30 mL/min. The carrier gas was passed through a moisture trap and an oxygen trap (Alltech) before entering the system. The gases of interest in the order of their expected elution times were N<sub>2</sub>, O<sub>2</sub>, CO, NO, CO<sub>2</sub>, N<sub>2</sub>O and NO<sub>2</sub>. The GC oven was operated at 30°C for 7 min to separate N<sub>2</sub>, O<sub>2</sub>, CO and

NO, then ramped at 20°C/min to 80°C to elute CO<sub>2</sub>, N<sub>2</sub>O and NO<sub>2</sub>. A 10-port valve (Valco) was installed in the GC so that experiments from two separate reactor systems can be alternately monitored, as shown in Figure 8. In position I, gas from reactor system A continuously passed through sample loop A, while gas from sample loop B was introduced into the GC column. Switching to position II directed the contents of sample loop A into the column and refilled sample loop B with the effluent from reactor system B. Using sample loop volumes of 1 or 2 mL was sufficient for the concentrations of gases used in this project. Performance of the catalysts was determined by comparing the GC and MS peak areas for the gas stream before and after the reactor. Peak areas were determined using commercially available software (PeakFit, Jandel).

## B. Catalyst Performance

The temperature dependence of catalyst activity is fundamental information that is needed of any catalyst. Therefore, performing experiments as a function of temperature, for preferred catalysts, comprised an important part of the overall program. The first catalyst evaluated as such was Catalyst 102. A plot of NO decomposed over this catalyst as a function of temperature is shown in Figure 9. These data show a maximum in activity at 500°C, at a space velocity of 50,000 h<sup>-1</sup>, in 16 percent O<sub>2</sub> and **absent added reductant** (hydrocarbon or CO). N<sub>2</sub>O was not detected under these conditions. A small amount of NO<sub>2</sub>, which never exceeded 2.6 ppm, was detected over this temperature range. Results of these measurements strongly suggest direct decomposition to N<sub>2</sub> and O<sub>2</sub>. The inclusion of 1000 ppm CO in the feed resulted in slight enhancement of activity. With CO, activity corresponded to removal of 10 percent NO at this same space velocity and at 1000°C, pointing to some reduction of NO by CO. The influence of added CO was further investigated as a function of space velocity at 1000°C. These data are shown in Figure 10. As expected, the plot shows a decrease in NO decomposition with increased space velocity. Most encouraging, however, is that appreciable activity was obtained even at this temperature and up to 250,000 h<sup>-1</sup>.

Dependence on space velocity at 500°C is shown in Figure 11. These data show 63 percent conversion at 50,000 h<sup>-1</sup> and 26 percent at 500,000 h<sup>-1</sup> (residence time: 7.2 ms). This is

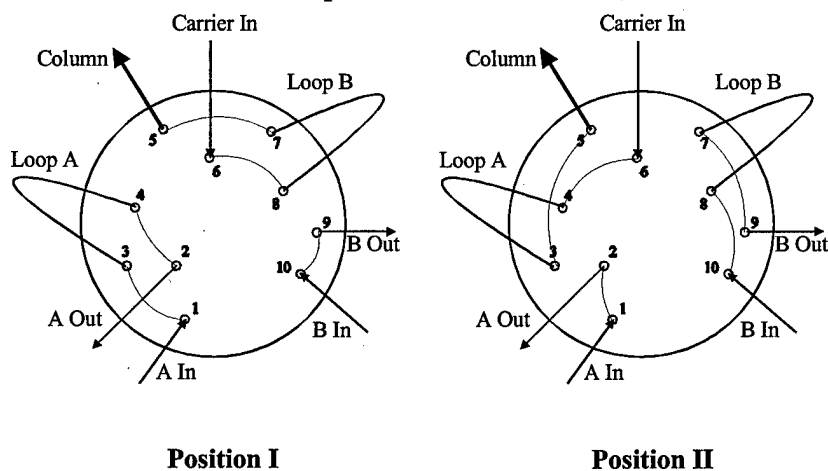


Figure 8. Schematic of the GC 10-port sampling valve.

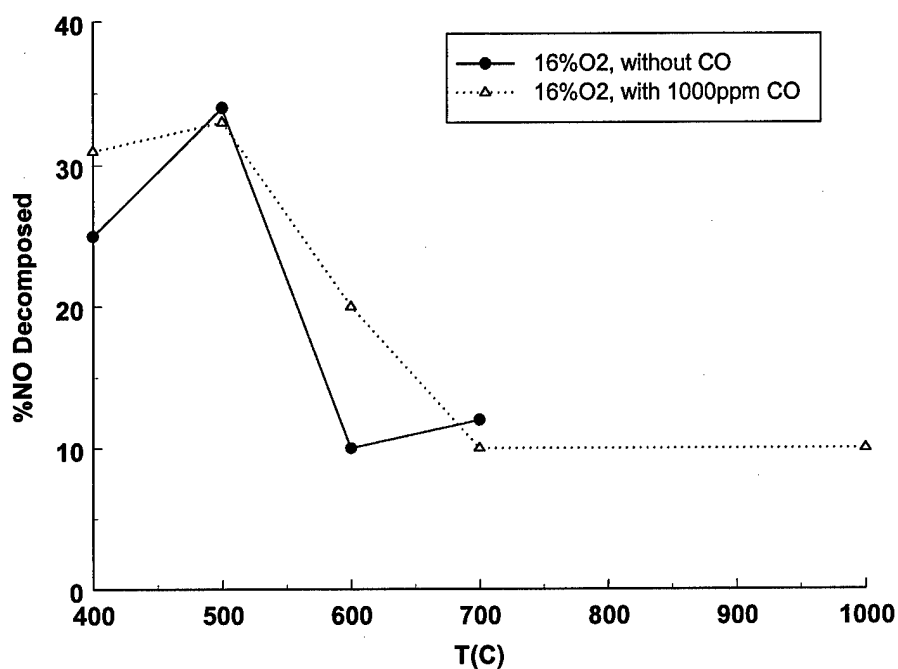


Figure 9. Plot of NO decomposed over Catalyst 102 versus temperature. GHSV = 50,000 h<sup>-1</sup>. 1000 ppm NO, 16% O<sub>2</sub>.

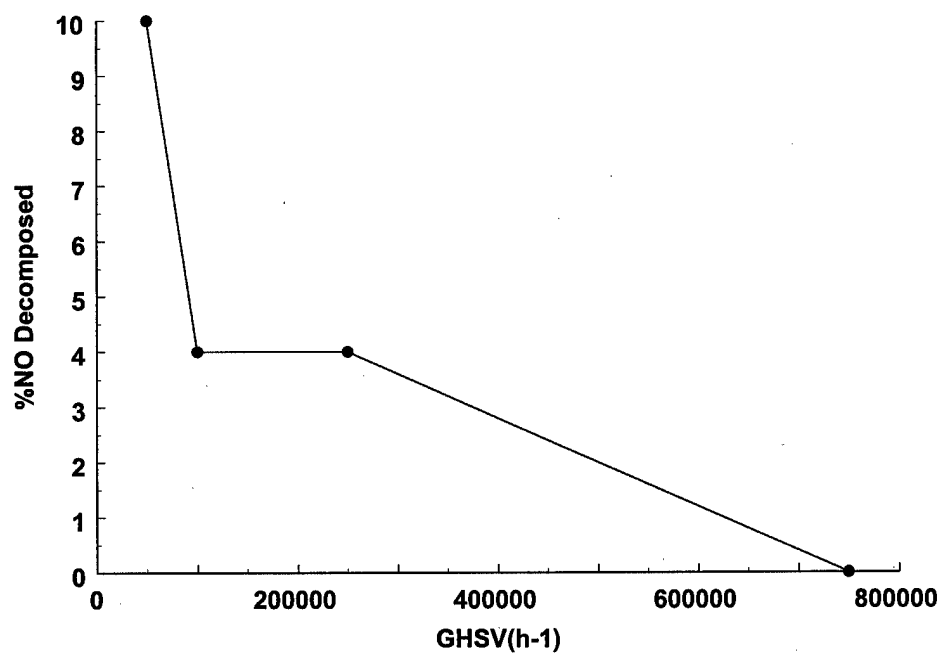
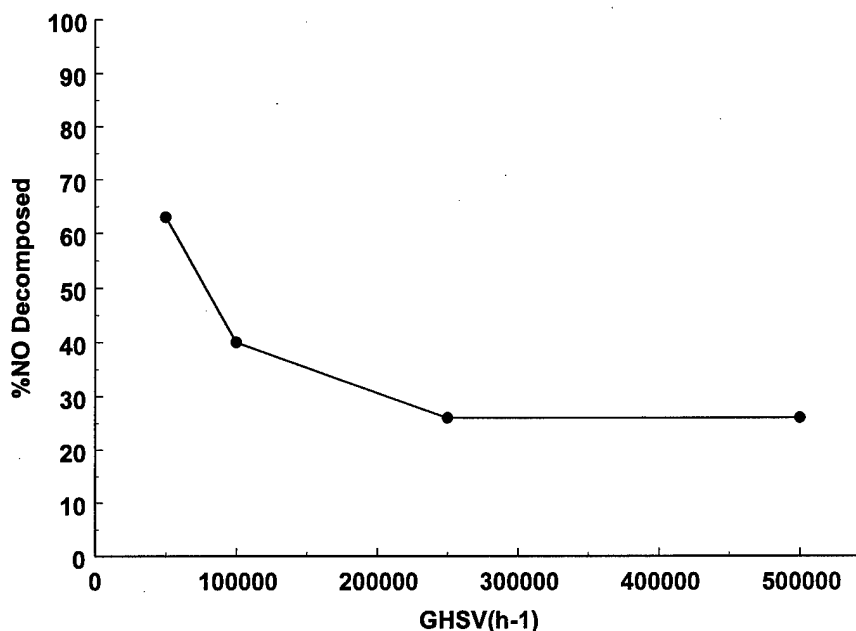


Figure 10. Plot of NO decomposed over Catalyst 102 versus space velocity for 1000 ppm NO in 16% O<sub>2</sub>. 1000 ppm CO. T=1000°C.



**Figure 11.** Plot of NO decomposed over Catalyst 102 versus space velocity for 1000 ppm NO, 16% O<sub>2</sub>. T=500°C.

clearly a significant activity level at the space velocities of concern.

The catalyst appeared to tolerate temperature excursions well. For example, returning to 500°C, activity of 24 percent versus 34 percent was observed. The CO<sub>2</sub> tolerance of the catalyst was exceptional: introduction of CO<sub>2</sub> to produce a reaction mixture 1000 ppm in NO, 16 percent O<sub>2</sub>, and 10 percent CO<sub>2</sub> resulted in NO decomposition of 25%. This strong tolerance to CO<sub>2</sub> tolerance may arise from the interaction between the base and acidic species present in the material. Whatever the case, tolerance to CO<sub>2</sub> is essential for a catalyst containing strongly basic species such.

The catalyst above was also found to possess significant oxidation activity towards hydrocarbons. A stream 1000 ppm in NO, 16 percent in O<sub>2</sub>, and 1000 ppm in propane gave about 15 percent removal of C<sub>3</sub>H<sub>8</sub> at 500°C and about 91 percent at 600°C at a GHSV of 22,000. The product was apparently CO<sub>2</sub>, although this was difficult to quantify using mass spectrometry, the analysis technique being used for these experiments.

Catalyst 102 was found, upon preparation by calcination of the component metal oxides and carbonates, to possess an XRD fingerprint characteristic of a single-phase material (Figure 12). Comparison of Figures 12 and 13 show that Bragg reflections initially present were persistent after running experiments at 500 and 600°C with 1000 ppm NO and 16 percent O<sub>2</sub> as well as with 1000 ppm propane for 18.5 hours. However, additional reflections appear, suggesting some reaction of the material. Significant changes in the X-ray emission spectra of the catalyst were not evident.

Catalyst 104, prepared by calcination of component oxides and carbonates at 750°C was found most probably to be multiphase (Figure 14). Again, experiments relating to temperature dependence of catalyst activity were performed as shown in Figure 15. As for the previous

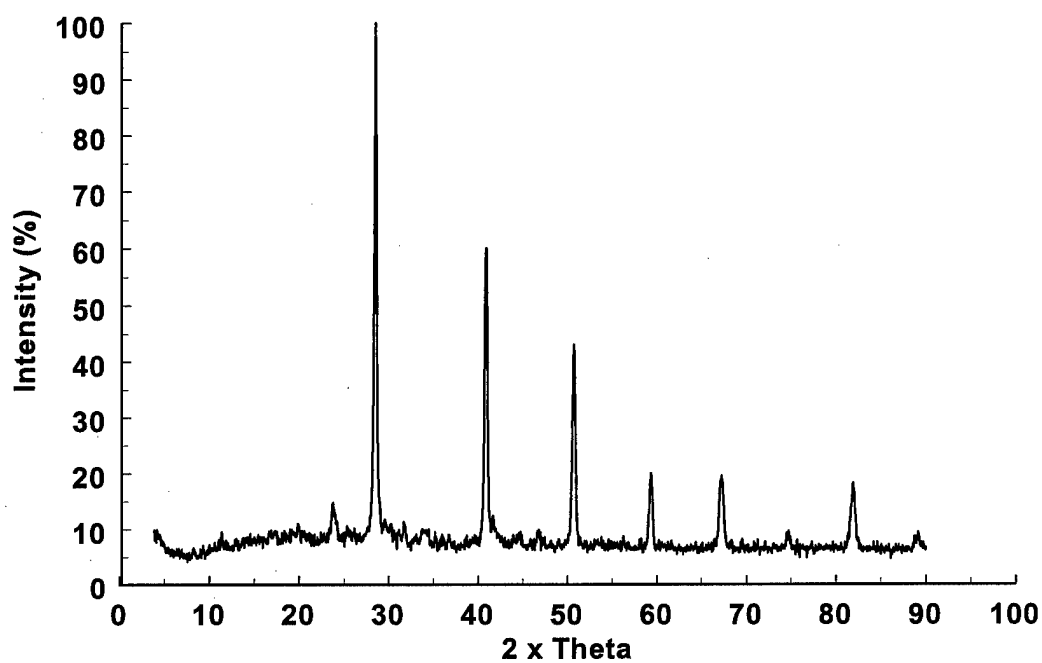


**Figure 12.** X-ray diffraction pattern of Catalyst 102 prepared by calcination of oxides at 1000°C for 4 hours.

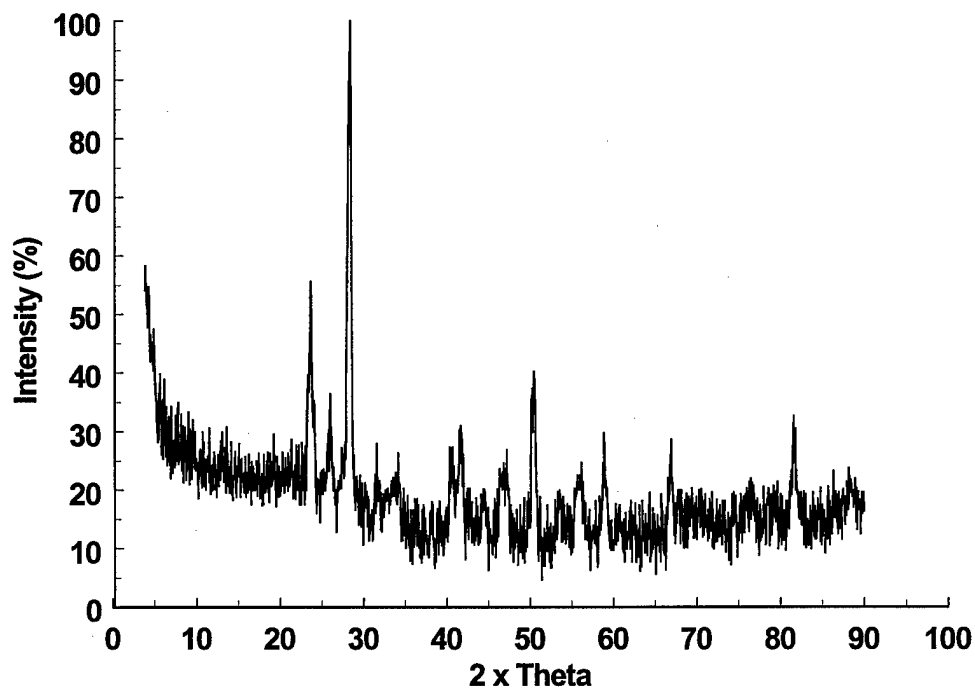


**Figure 13.** X-ray diffraction pattern of Catalyst 102 after 18.5 hours online.

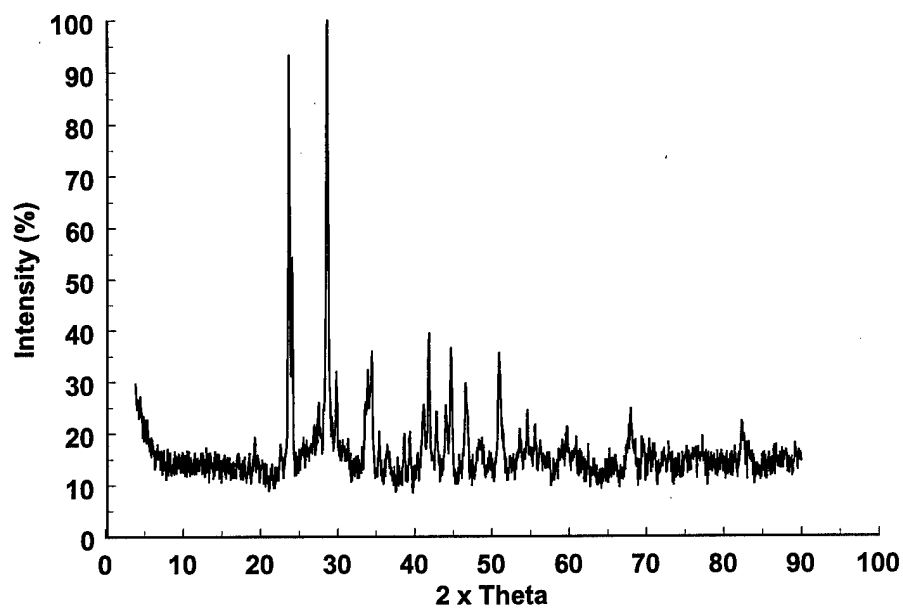


Figure 14. XRD pattern of Catalyst 104 prepared from the oxides.

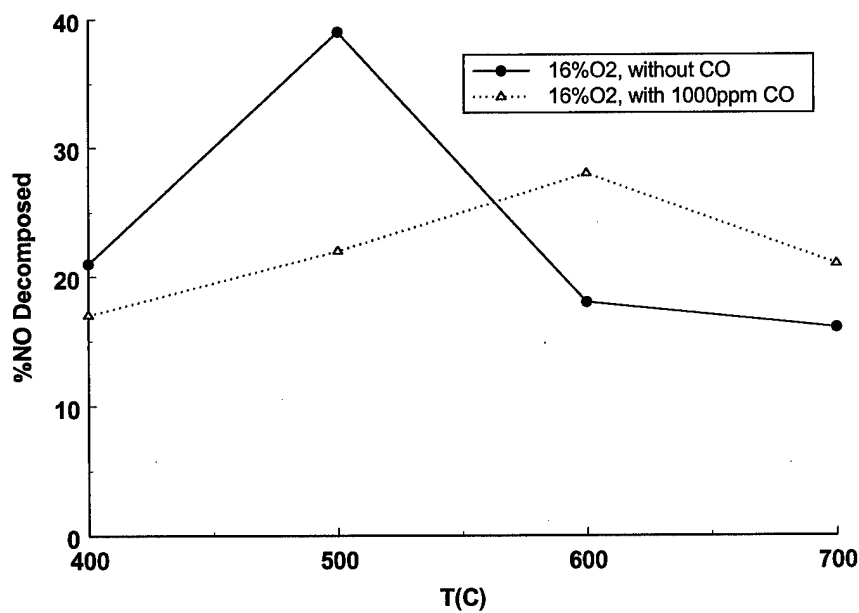


Figure 15. NO decomposed over Catalyst 104 versus temperature. 1000ppm NO, 16%O<sub>2</sub>. GHSV = 50,000 h<sup>-1</sup>.

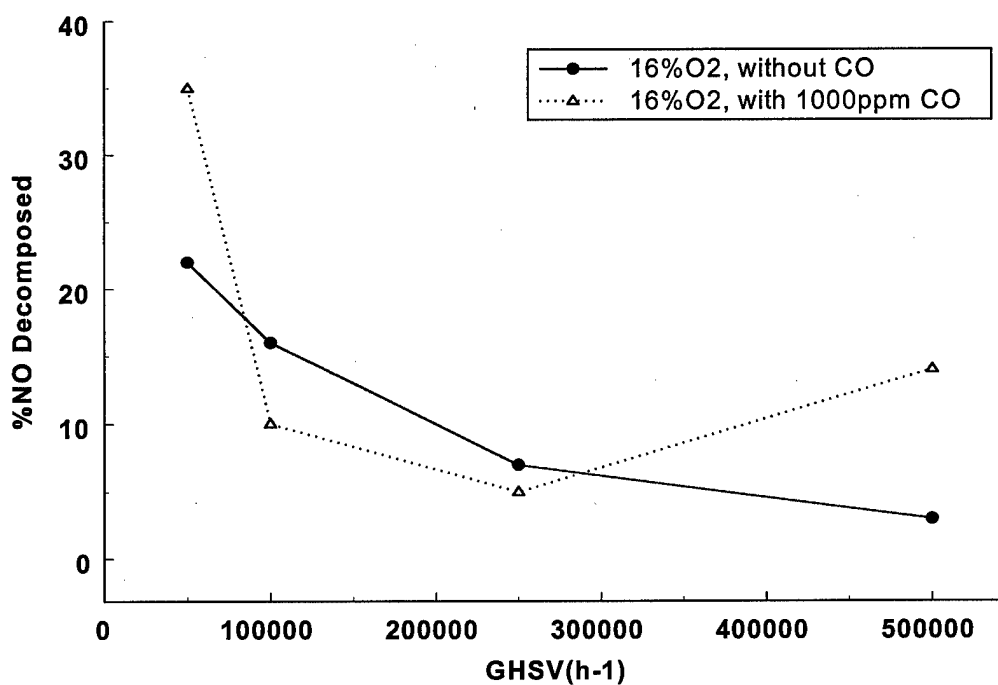


Figure 16. NO decomposed over Catalyst 104 versus space velocity.  
 $T=500^{\circ}\text{C}$ . 1000 ppm NO, 16% O<sub>2</sub>.

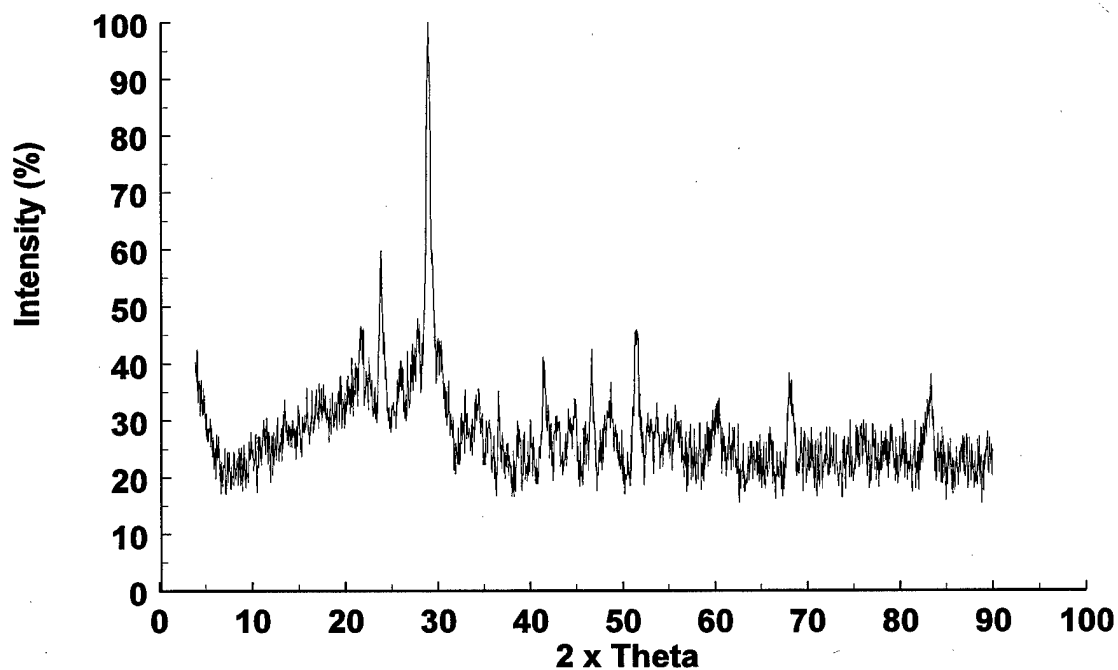


Figure 17. XRD pattern of Catalyst 104 after 4.5 hours on line.

catalyst, data for this catalyst show enhancement of activity at higher temperatures by carbon monoxide in the feed. However, once again, the catalyst was quite active even absent CO. Space-velocity dependence is shown in Figure 16. After experiments (see Table 5) with this material, XRD showed some change, the original reflections remaining, but with some additional low-angle reflections (Figure 17). EDX spectra showed an increase in the intensity of the line corresponding to the basic species after subjecting the catalyst to a similar experimental regimen as Catalyst 102, but for only 4.5 hours. This catalyst showed less combustion activity than Catalyst 102. At a space velocity of only  $2810 \text{ h}^{-1}$ , 6 percent of 1000 ppm  $\text{C}_3\text{H}_8$  was removed at  $500^\circ\text{C}$ . Oxidation of propane was complete, however, at  $750^\circ\text{C}$ .

The most-promising material studied during Phase I was Catalyst 105. This material appeared to be predominantly a single phase, with a small fraction of some other phase present (Figure 18). A preliminary crystallographic assignment was made to this powder pattern: an orthorhombic unit cell with lattice constants  $a = 5.90\text{\AA}$ ,  $b = 16.3\text{\AA}$ , and  $c = 5.86\text{\AA}$ . The material probably possesses the brownmillerite structure, based on the assigned stoichiometry. The material showed appreciable propylene oxidation activity. At  $500^\circ\text{C}$  and  $50,000 \text{ h}^{-1}$ , 1000 ppm of  $\text{C}_3\text{H}_6$  in the gas stream was completely converted. Under the same conditions, but with 1000 ppm CO replacing propylene, 66 percent of the CO was converted. After approximately 1.5 hours on line, diffraction pattern showed essentially no change (Figure 19). Although considerably different on line times were employed with Catalysts 102, 104, and 105 just described, it would appear from these data that Catalyst 105 was most stable under the various conditions encountered. Consideration of EDX spectra for the material supports this view. Essentially no difference was evident from consideration of spectra obtain before and after experiments other than the appearance of the Al line, arising from the sample holder.

Temperature dependence of catalyst activity is shown in Figure 20, both with and without added CO. Again, very substantial decomposition of NO was obtained. No evidence of  $\text{N}_2\text{O}$  was observed.  $\text{NO}_2$  comprised less than 1% of the product stream (ppm levels). The inclusion of CO in the stream resulted in enhanced activity at higher temperatures. The space-velocity dependence of activity at  $1000^\circ\text{C}$  with CO is shown in Figure 21. Even at this higher temperature, measurable activity was obtained at up to  $250,000 \text{ h}^{-1}$ . At  $500^\circ\text{C}$ , significant activity (14 percent removal) was obtained at up to  $500,000 \text{ h}^{-1}$ , **absent any added reductant** (Figure 22).

The activity of this catalyst decreases at higher temperatures because the generation of an adsorbed  $\text{NO}_2$  intermediate becomes less favorable. However, two points concerning this issue should be made here: 1) no appreciable levels of gas-phase  $\text{NO}_2$  were generated and 2) increasing catalyst dispersion (surface area) overcame temperature limitations to a degree. This second point will be amplified in Task 3, where data for Catalyst 105 supported on yttria-stabilized zirconia (YSZ) powder is presented. A plot of the entire temperature range studied is shown in Figure 23. The data show a rather sharp maximum in activity at  $400^\circ\text{C}$ . However, very significant activity was evident at  $500^\circ\text{C}$ . Although this is probably at the lower end of the temperature range for gas turbine exhausts, application in the exhausts of diesel and lean burn engines as well as in those of large specialty engines such as natural gas prime movers would appear to be good alternative applications. As indicated previously, and as will be demonstrated in Task 3, increased dispersion of the catalyst resulted in much greater activity towards  $\text{NO}_x$  decomposition at these higher temperatures.

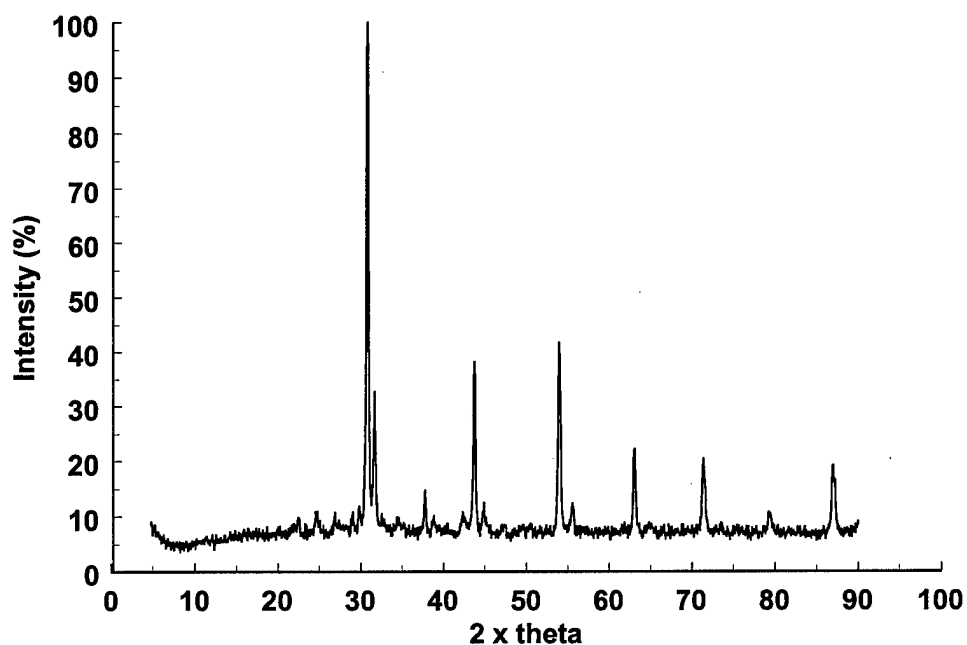


**Figure 18.** XRD pattern of Catalyst 105 prepared by calcination of metal oxides at 1000°C.

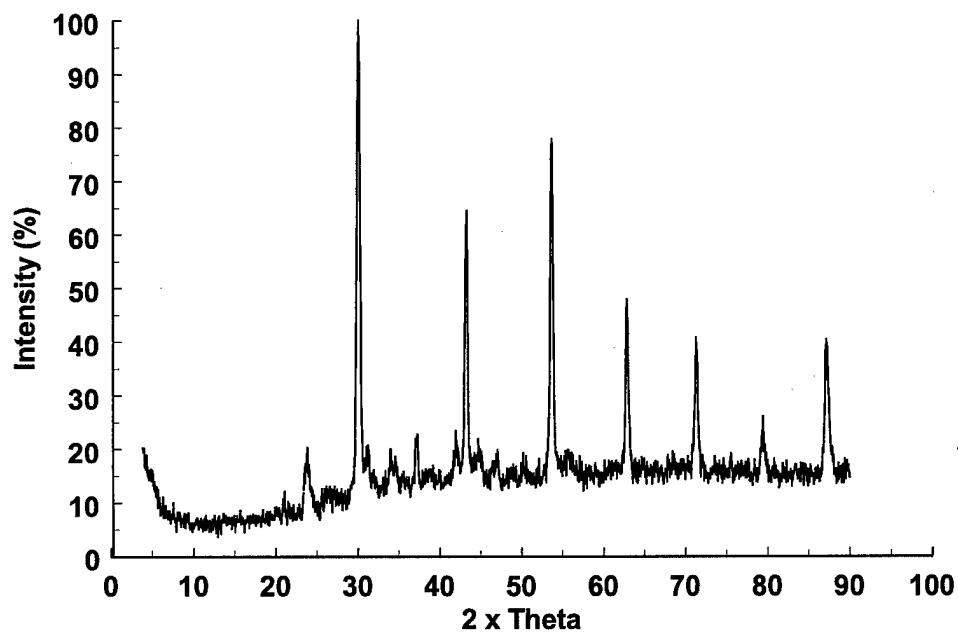


**Figure 19.** XRD pattern of Catalyst 105 after 1.5 hours on line.

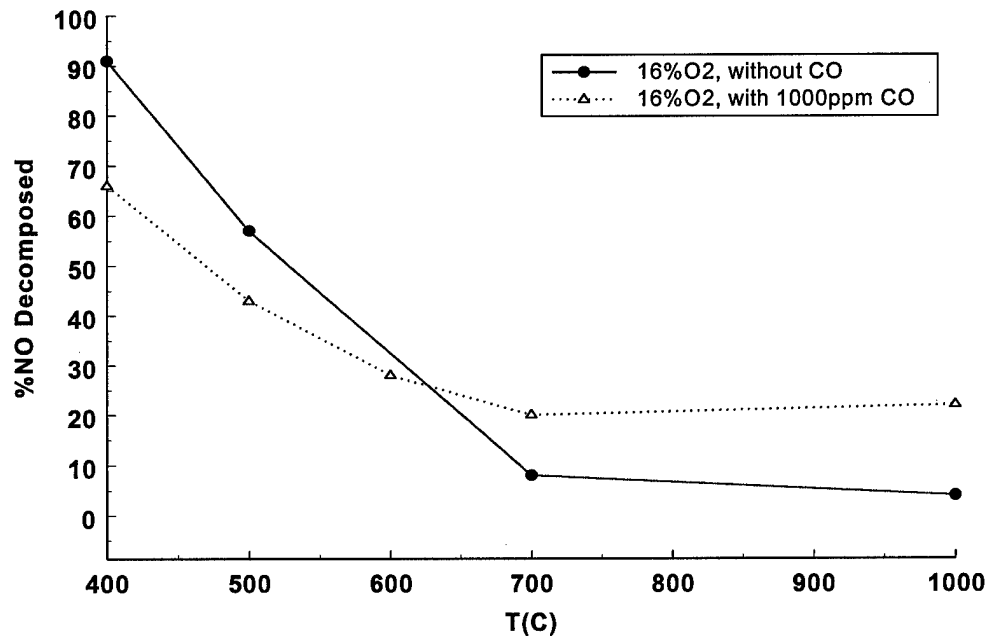


Figure 20. NO decomposition versus temperature for Catalyst 105. GHSV = 50,000 h<sup>-1</sup>. 1000 ppm NO, 16% O<sub>2</sub>.

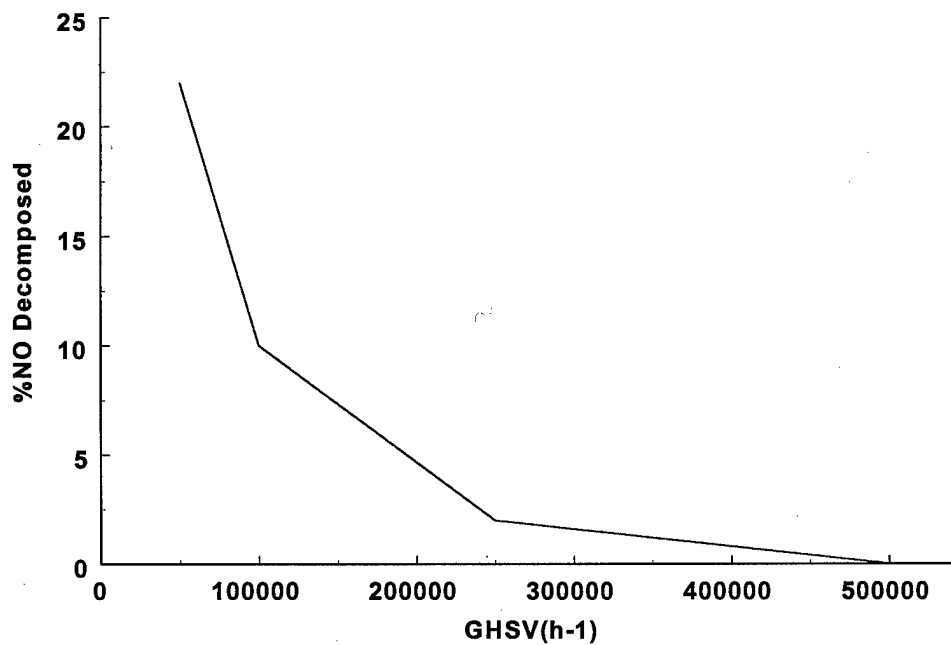


Figure 21. NO decomposed versus space velocity for Catalyst 105. T=1000°C. 1000 ppm NO. 16% O<sub>2</sub>. 1000 ppm CO.

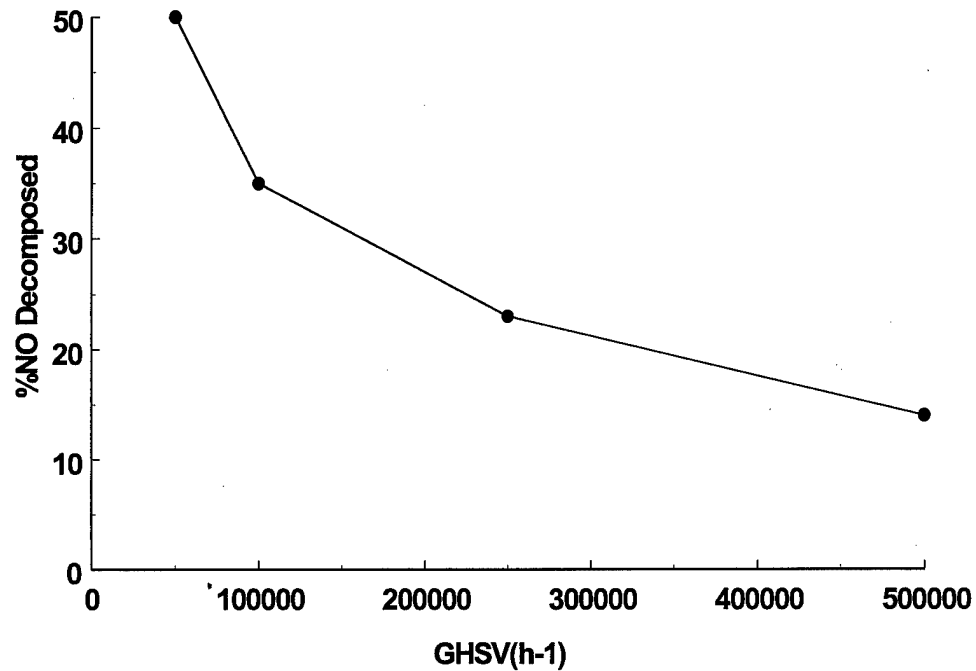


Figure 22. NO decomposed over Catalyst 105 versus GHSV.  $T=500^{\circ}\text{C}$ . 1000 ppm NO, 16%  $\text{O}_2$ .

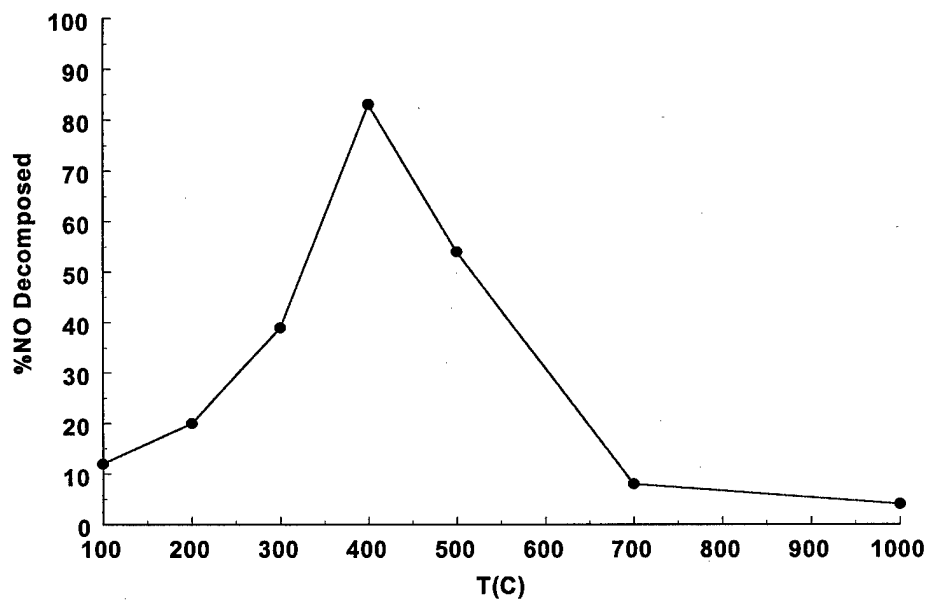


Figure 23. Plot of  $\text{deNO}_x$  activity of Catalyst 105 versus temperature.  $\text{GHSV} = 50,000 \text{ h}^{-1}$ . 1000 ppm NO, 16%  $\text{O}_2$ .

Some insight into the nature of the process occurring here is in order. Figure 24 shows data for the dependence of NO removal on oxygen concentration. Between 8 and 16 percent  $O_2$ , little difference in activity was observed. However, in the absence of oxygen, the catalyst was inactive. This supports the view that an oxidized intermediate is involved in the overall mechanism. Conversion, however, appeared to depend on NO level (Figure 25). Between 500 and 1000 ppm, the dependence was not very strong, but below 500 ppm, activity dropped more rapidly. This points to kinetic issues involving NO concentration. If the intermediate involved is  $NO_2$ , then the kinetic limitation actually involves the surface coverage of  $NO_2$ . It is this kinetic limitation that must be addressed in improving overall conversion.

Initial longevity tests of this catalyst have been quite remarkable. Activity was essentially preserved over 140 hours of operation (Figure 26). Increasing the space velocity from  $50,000\text{ h}^{-1}$  to  $500,000\text{ h}^{-1}$  resulted in persistent (6 hours, see Figure 27) NO conversion greater than that shown in Figure 22. It is not clear whether this is due to actual improvement in activity or variance between samples. The latter could easily be explained in terms of between-sample variation in catalyst dispersion. As will be shown in Task 3, increased catalyst dispersion resulted in much higher catalytic activity. Another possible explanation is that attainment of an increased level of some surface intermediate occurs over this time. In any event, the persistence of activity demonstrated indicates that poisoning by surface nitrates does not occur.

The introduction of 10 ppm  $SO_2$  and 10 percent  $CO_2$  in the feed did not cause statistically significant reduction in the activity of the material over a period of 3 hours. For example, after 3.5 hours with these species in the simulated exhaust stream,  $NO_x$  conversion was 43 percent versus 44 percent prior to the introduction of  $CO_2$  and  $SO_2$ .

The last catalyst to be considered was Catalyst 98. Data for this material presented in Table 5 show exceptional activity. An analog of this material, Catalyst 93, which was prepared by coprecipitation, also showed exceptional activity. In fact, at  $783,000\text{ h}^{-1}$ , mass spectrometry showed a transient in  $NO_x$  removal of about 35 percent and persistent activity of about 12 percent conversion at  $500^\circ\text{C}$ . However, the predominant product was  $N_2O$ . It was the occurrence of this product that led to the development of the other three catalysts (102, 104, and 105).

Coprecipitated Catalyst 93 material was found to almost completely burn propylene at  $500^\circ\text{C}$ : 96 percent of 1000ppm propylene was removed. At  $600^\circ\text{C}$ , combustion was complete. The only product in either case was  $CO_2$ .

The relative merits of these four catalysts are summarized in Table 7, which suggests that Catalyst 105 is the best material studied to date in Phase I. Factors contributing to the catalyst's activity are not entirely clear at this point. However, one possible scenario will be presented here. The mechanism previously described in this document, involves participation of the basic cation as an adsorption site for  $NO_2$  generated by oxidation at the transition-metal cation sites.  $NO_2$  generated as such is very reactive both because of the Lewis base (electron donating) nature of the base cation and the presence of transition-metal ions in the vicinity of adsorbed  $NO_2$  or other such oxidized species. It must also be emphasized here that the apparent brownmillerite structure of the material provides intrinsic oxygen ion vacancies that can serve as Lewis acid sites for basic oxygen ions, further aiding in the dissociation of the surface intermediate. Brownmillerite catalysts such as  $Sr_2Fe_2O_5$  have previously been demonstrated by other workers where they have shown<sup>4</sup> significant activity at low space velocities.

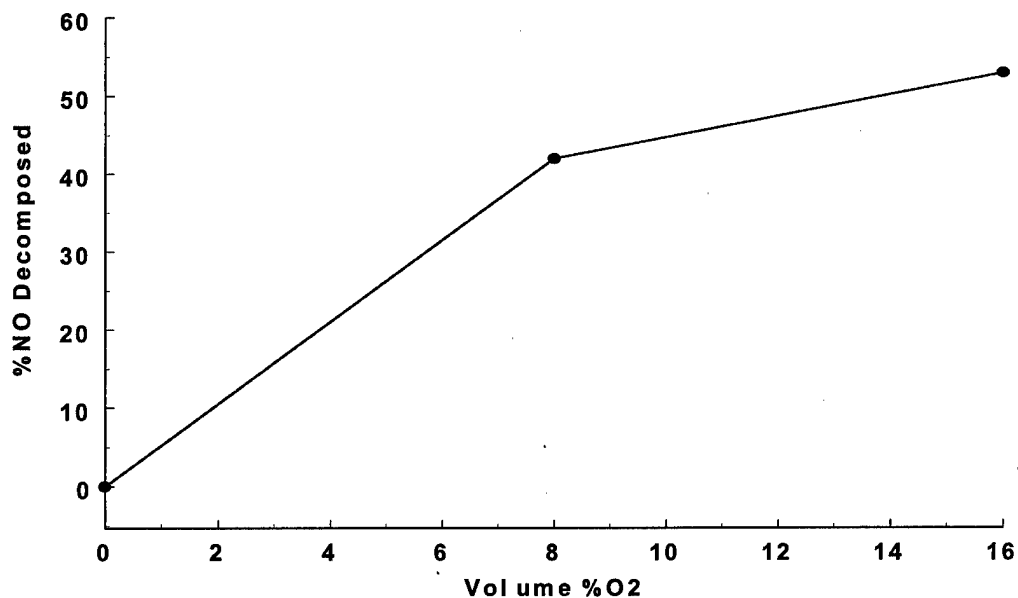


**Figure 24.** Plot of NO decomposed over Catalyst 105 versus oxygen content of stream.  $T=500^{\circ}\text{C}$ .  $\text{GHSV}=50,000\text{ h}^{-1}$ . No reductant was present in the feed.

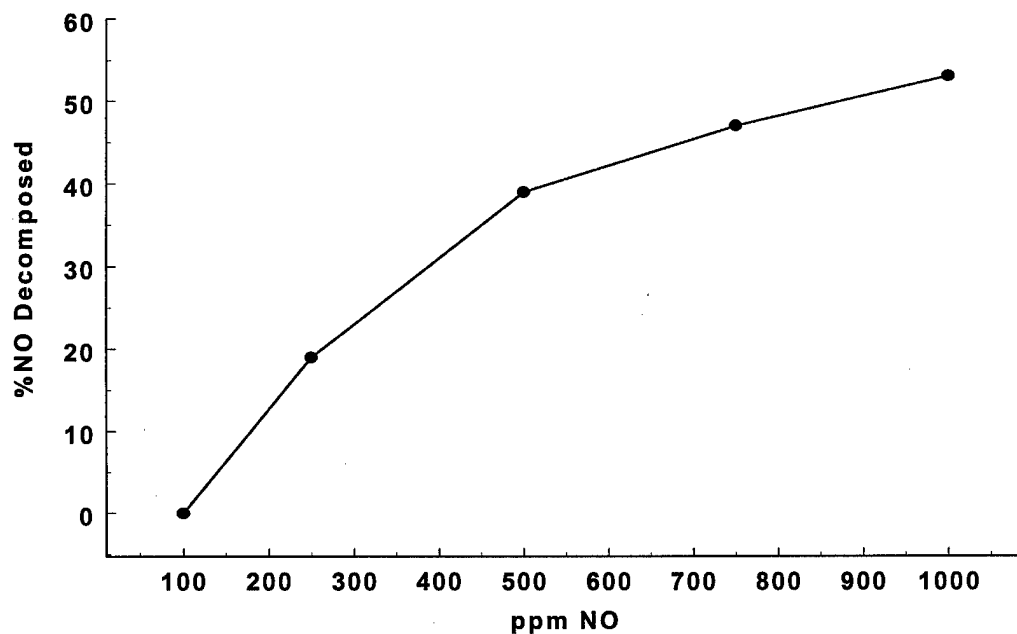


**Figure 25.** NO decomposed over Catalyst 105 as a function of NO concentration.  $T=500^{\circ}\text{C}$ . 16%  $\text{O}_2$ .  $\text{GHSV}=50,000\text{ h}^{-1}$ . No reductant was present in the feed.

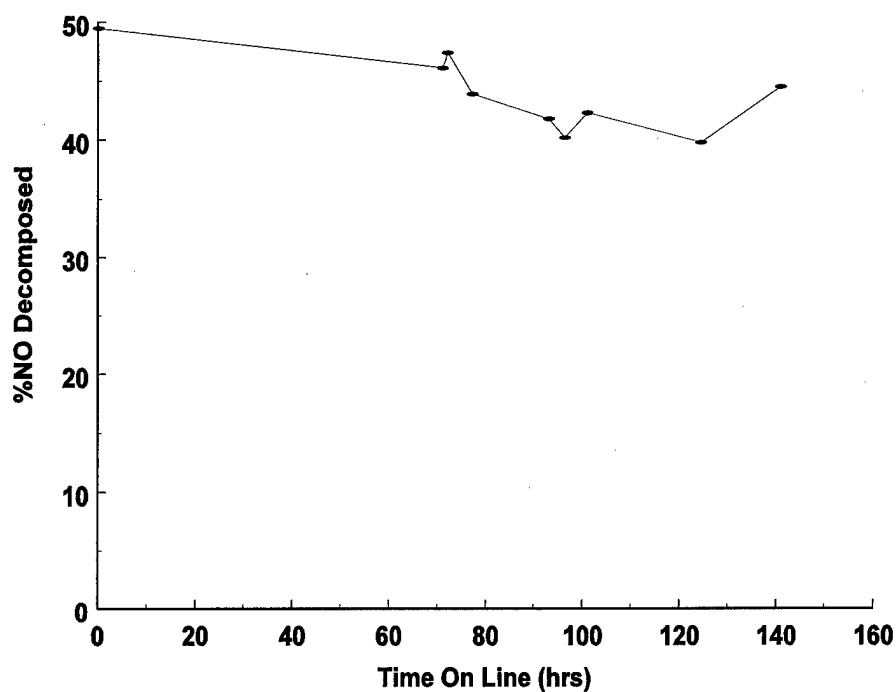


Figure 26. Plot of deNO<sub>x</sub> activity for Catalyst 105 versus time on line. T=500°C. GHSV=50,000 h<sup>-1</sup>. 1000 ppm NO, 16% O<sub>2</sub>.

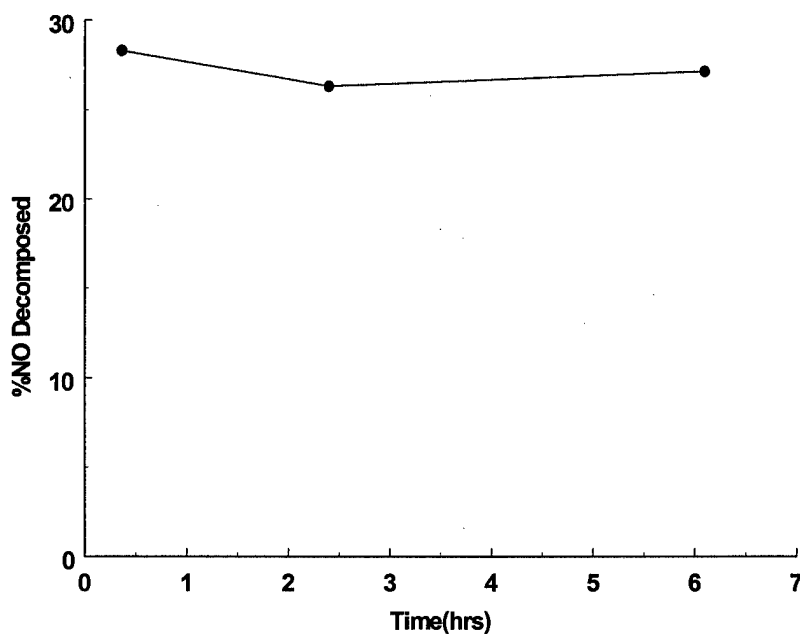


Figure 27. Plot of deNO<sub>x</sub> activity for Catalyst 105 versus time on line. GHSV = 500,000 h<sup>-1</sup>. 1000 ppm NO, 16% O<sub>2</sub>.

**Table 7.**  
**Summary of Data for Preferred Catalysts Studied During Phase I. All Data with 16% O<sub>2</sub>, 500ppm NO in the Absence of an Intentionally Introduced Reductant**

Catalyst	Highest GHSV Examined	Residence time	%NO Decomposed at 500 °C at Highest GHSV	Anticipated Chemical/Thermal Stability	BET Surface Area (m <sup>2</sup> /g)	CO <sub>2</sub> (10%) Tolerance	SO <sub>2</sub> (10ppm) Tolerance	Time On line/ (hrs) Activity Remaining (%)	N <sub>2</sub> O/NO <sub>x</sub> in Products	Hydrocarbon Combustion Activity
Catalyst 105	500,000	7.2	27	high	0.63	very high (3.5 hrs- no activity loss)	very high (3.5 hrs without activity loss)	140 hrs/88	trace levels (<1% of products)	100% of 1000 ppm C <sub>3</sub> H <sub>8</sub> at 66% of 1000 ppm CO <sub>2</sub> at 500 °C and 50,000 h <sup>-1</sup>
Catalyst 102	500,000	7.2	26	high	0.60	no loss of activity	not tested	71 hrs/59	trace levels (<1% of products)	91% of 1000 ppm C <sub>3</sub> H <sub>8</sub> at 600 °C and 50,000 h <sup>-1</sup>
Catalyst 93	783,000	4.6	14	low unless supported K migration	2.55	not tested	not tested	not tested	products 50-80% N <sub>2</sub> O	96% of 1000 ppm C <sub>3</sub> H <sub>8</sub> at 500 °C and 50,000 h <sup>-1</sup>
Catalyst 104	500,000	7.2	12	moderate at <700 °C	0.58	no loss of activity	not tested	26 hrs/56	trace levels (<1% of products)	100% of 1000 ppm C <sub>3</sub> H <sub>8</sub> at 750 °C and 2810 h <sup>-1</sup>

The overall surface binding energy of oxygen on the surface of the catalyst is such as to promote a high desorption rate of oxygen evolved by decomposition of the surface intermediate and to regenerate vacant sites. The oxidized forms of transition-metal species would then have to be regenerated by interaction with NO (i.e., Mars - van Krevelen mechanism).<sup>5</sup> This scenario seems to be consistent with experimental observation: increased exhaust oxygen content increases the NO decomposition rate. Thus, **oxygen serves not to inhibit the decomposition reaction, but to promote it.** This is remarkably different to other approaches, such as those employing metal ions incorporated into zeolite materials. In that case, reagentless activity relies on local electric fields in the zeolite framework permitting continuous regeneration of active oxidation states of Cu or other metal cations, and consequently, permitting the continuous desorption of oxygen. This approach<sup>6</sup> has not been particularly successful, however. Activity at only a few hundred reciprocal hours has been demonstrated.

The potential issue of poison tolerance can be addressed here by reference to other work,<sup>7</sup> which showed that tolerance of perovskite materials such as  $\text{LaCoO}_3$  was strongly improved by doping with species such as Sr, Ti, Zr, and cations of a few other metals. It is certain that whatever  $\text{SO}_2$  intolerance in Catalysts 102, 104, and 105 that might arise (i.e., at levels higher than 10 ppm) can be mitigated by small perturbations in composition analogous to those of reference 6. More significant will be the problem of improving catalyst dispersion, as was amply demonstrated in Task 3.

### *Task 3      Selection and Performance Testing of Supported Catalysts*

In this task, the objective was to incorporate preferred catalysts onto support materials. Three such supports were employed: Cordierite monolith, alumina (neutral Brockmann) powder, and yttria-stabilized zirconia powder. The latter two materials are certainly of greater relevance to the problem at hand, but were not available in monolith form. Procedures for incorporation of catalysts onto each of these supports will now be described.

Solutions of metal nitrates were prepared with constituents in the appropriate molar ratios so as to prepare the equivalent of 0.33M Catalyst 105 and 0.5M Catalyst 98 Cordierite monoliths were prepared by simply introducing separate pieces of 400 rectangular cell/in<sup>2</sup> cordierite honeycomb monolith (Corning) of dimensions 1 cm diameter by 0.4, 0.7, or 1.0 cm length in the above solutions, oven drying at 110°C, followed by calcination at 400°C (for Catalyst 98) or 1000°C (for Catalyst 105). Powders were prepared by adding just enough powder ( $\text{Al}_2\text{O}_3$  or YSZ) to a small volume (5 ml) of metal nitrate solution to produce a thick slurry. Oven drying of the powders at 110°C was followed by calcination at 400 and 1000°C for Catalyst 98 and Catalyst 105, respectively. Powders were screened in the same manner as unsupported catalysts described in Task 1.

Data for the space velocity dependence of activity of YSZ-supported Catalyst 105 (4.3 wt%) is presented in Figure 28 at 500 and 700°C. The data show an unexpectedly mild dependence on residence time. The reason for this is not clear. A rate limiting surface equilibrium is one possible explanation.  $\text{DeNO}_x$  was quite expectedly greater at the lower temperature. **The other key observation here is the magnitude of activity: 35 percent conversion at a space velocity of  $10^6 \text{ h}^{-1}$ . This is amazingly high for any reaction, but even more astonishing for reagentless decomposition of nitrogen oxides in an  $\text{O}_2$ -rich stream.** Even the 11 percent obtained at 700°C and the same space velocity was remarkable. After taking into account the

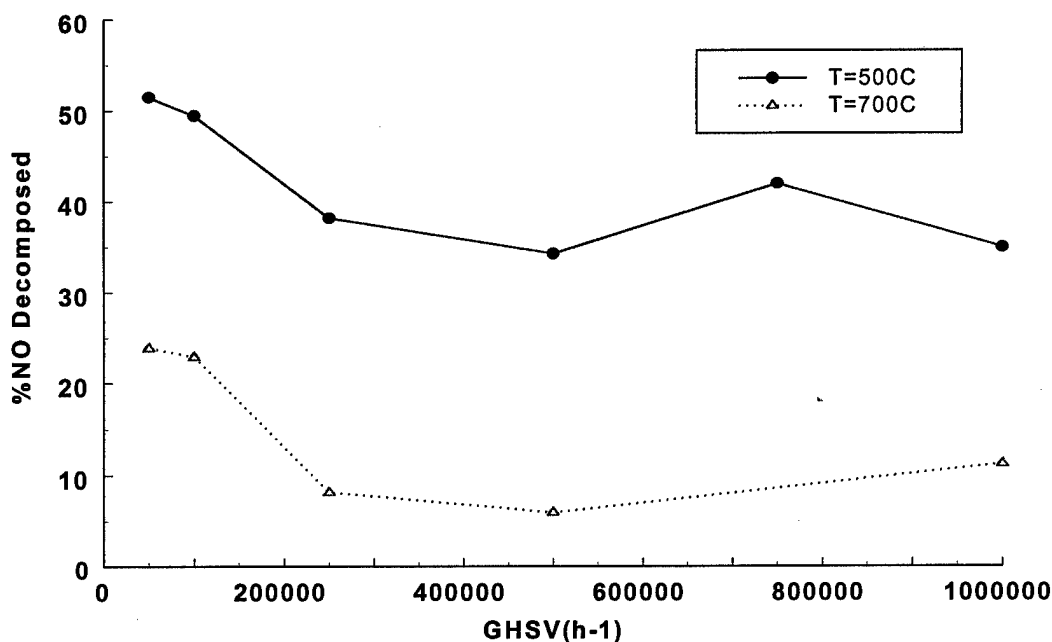


**Figure 28.** Plot of deNO<sub>x</sub> over Catalyst 105 (4.3 wt%/YSZ) versus space velocity. NO concentration: 1000 ppm up to 250,000 h<sup>-1</sup>, 953 ppm at 500,000 h<sup>-1</sup>, 636 ppm at 750,000 h<sup>-1</sup>, and 477 ppm at 1,000,000 h<sup>-1</sup>. 16% O<sub>2</sub>. BET surface area = 2.5 m<sup>2</sup>/g. Weight catalyst used: 0.025g.

catalyst loading (4.3 wt%), these results were actually obtained with only 1 mg of catalyst.

Supporting Catalyst 98 on YSZ resulted in the data shown in Figure 29. Conversion ranged between 32 and 44 percent over this period, less than that for the YSZ-supported Catalyst 105.

Both of these catalysts were supported also on Cordierite (a magnesium aluminosilicate) honeycomb monolith. Data for Catalyst 98 (loading: 0.313 g) on a 1 cm-long Cordierite monolith is presented in Figure 30. The data show no deterioration in activity over 65 hours operation at 500°C and space velocity of 15,000 h<sup>-1</sup> in an oxygen rich (16 percent), reductant-free atmosphere. In fact there may have been some increase in activity over the course of this experiment. There was some redistribution of catalyst over the monolith as well as some change in the catalyst chemical composition, as evidenced by EDX spectra. Comparison of spectra obtained before and after the experiment represented by Figure 33, shows that all lines associated with the catalyst increased relative to Al and Si lines. Additionally, there was a change in the relative intensities of the lines. The spectra indicate that a greater fraction of Lewis acid cation, relative to transition-metals was present in the catalyst. The ratio of base to transition-metals also appeared to increase, possibly explaining the increase in activity with time on line.

Catalyst 105 was also supported on a Cordierite monolith and evaluated. The data for space-velocity dependence obtained with a 0.4 cm-long Cordierite-monolith-supported Catalyst 105 (loading: 0.0272g) is presented in Figure 31. At 50,000 h<sup>-1</sup>, conversion was only 9 percent. This does not compare favorably with the YSZ supported material reported earlier. This was apparently due to bypass of the monolith by the gas stream. Increasing the length of the monolith

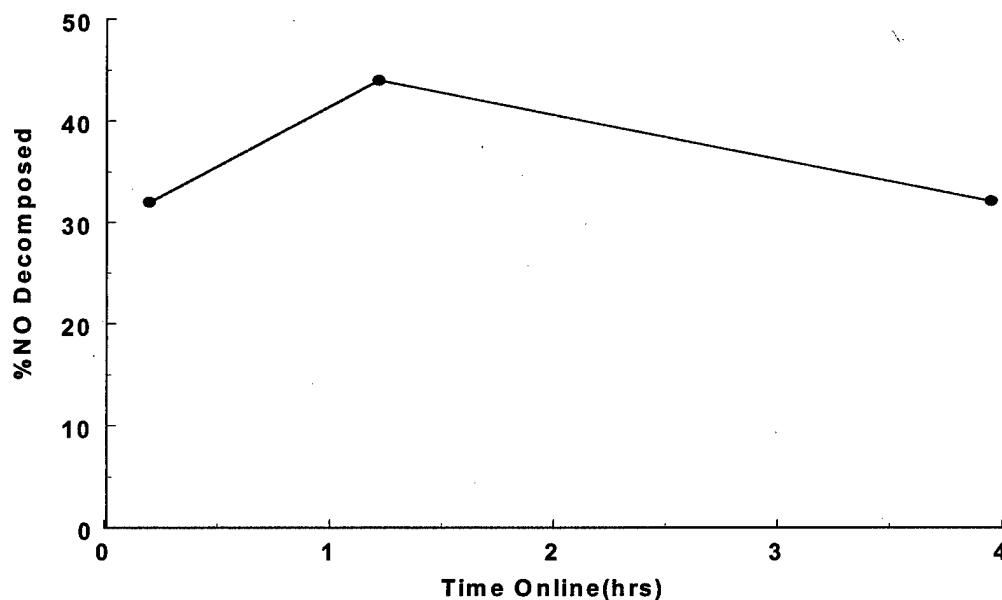


Figure 29. Plot of NO conversion versus time online for Catalyst 98 (3.2wt%)/YSZ.  $T=500^{\circ}\text{C}$ . 1000ppm NO, 16%  $\text{O}_2$ . GHSV = 50,000  $\text{h}^{-1}$ .

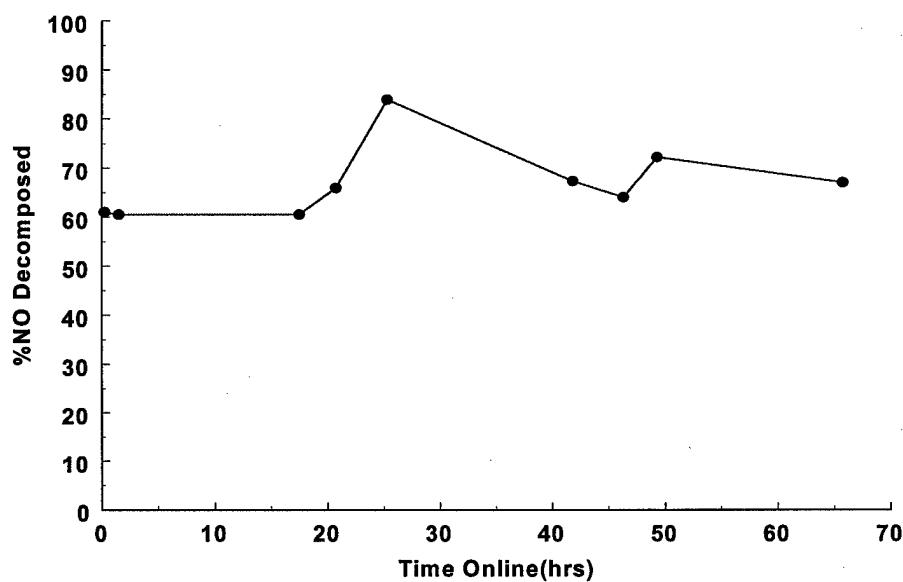
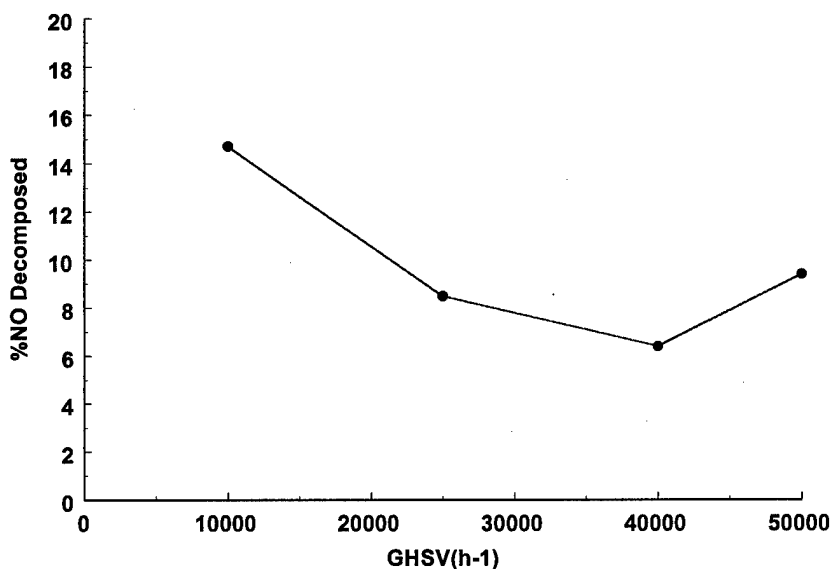


Figure 30. NO decomposed versus time for Catalyst 98 (0.313g) supported on 1cm long, 1cm diameter Cordierite monolith.  $T=500^{\circ}\text{C}$ . 1000ppm NO, 16%  $\text{O}_2$ . GHSV = 15,000  $\text{h}^{-1}$ .



**Figure 31.** NO decomposed versus space velocity for Catalyst 105 (loading: 0.027g)/cordierite monolith. T=500°C. NO concentration: 1000 ppm for 10,000 and 25,000 h<sup>-1</sup>, 625 ppm for 40,000 h<sup>-1</sup>, and 500 ppm for 50,000 h<sup>-1</sup>. 16% O<sub>2</sub>.

to 1 cm increased the overall loading to 0.070 g and the conversion to 21 percent (versus 8.5 percent for the 0.4 cm monolith). Thus, proportionality of conversion to surface area was demonstrated. On the basis of loading, the activity this supported catalyst is equal to or greater than that of supported Catalyst 98. EDX spectra showed nonuniform distribution of catalyst, with large areas being essentially absent catalyst.

In summary, results obtained in this task demonstrated the positive influence of increased catalyst dispersion on overall activity. This was demonstrated most convincingly by the material Catalyst 105 supported on YSZ. Using only 25 mg of the material (containing only 1 mg of catalyst), 35 percent of the NO in a stream 477 ppm in NO could be removed in the presence of 16 percent O<sub>2</sub>, at a space velocity of 10<sup>6</sup> h<sup>-1</sup> and temperature of 500°C, conditions quite consistent with those encountered in gas turbine exhausts.

#### IV. SUMMARY OF FINDINGS DURING PHASE I

- A series of 114 catalysts were successfully synthesized by ceramic processing, coprecipitation, and by impregnation of powdered supports. Prior to determining their activity towards NO<sub>x</sub> decomposition, we initially characterized these catalysts by X-ray diffraction (XRD) and surface area analysis by the Brunauer - Emmett - Teller (BET) method.
- Selected catalysts were initially evaluated for NO<sub>x</sub> decomposition activity at fixed space velocity. Temperatures were chosen according to the calcination temperature employed in their initial preparation. Significant measurable activity was obtained with the materials

$(\text{Bi}_2\text{O}_3)_{1-x}(\text{WO}_3)_x$ ,  $(\text{Bi}_2\text{O}_3)_{1-x}(\text{Nb}_2\text{O}_5)_x$ , and a basified catalyst (Catalyst 2b), using a feedstream containing 1000 ppm NO and absent any intentionally introduced oxygen.

- Activities for catalysts  $(\text{Bi}_2\text{O}_3)_{1-x}(\text{WO}_3)_x$  and  $(\text{Bi}_2\text{O}_3)_{1-x}(\text{Nb}_2\text{O}_5)_x$  were found to decrease with the amount of oxygen added, while that for the base coprecipitated Catalyst 2b was not affected by the presence of  $\text{O}_2$  at up to 16 volume percent **absent any added reagent** such as hydrocarbon or CO.
- Comparison of catalytic activity results obtained using basified Catalyst 2b with those obtained using Catalyst 2a made from the oxide suggested that base promotion was essential to simultaneously achieving both oxygen tolerance and high activity towards  $\text{NO}_x$  decomposition.
- Several catalysts anticipated to have greater thermal stability than coprecipitated catalysts were synthesized from the corresponding oxides. All of these materials were found to possess a single crystallographic phase, either from the fluorite structure or from the brownmillerite/perovskite structure. Thermal stability of the materials made from oxides was experimentally verified.
- Preferred catalysts were evaluated under conditions of fixed space velocity. All showed significant direct decomposition activity at  $50,000 \text{ h}^{-1}$  and  $500^\circ\text{C}$  in 16 percent  $\text{O}_2$ , **absent any introduced reagent**. These catalysts were also examined in the presence of propane, propylene, or CO as intentionally introduced reductants and were shown effective for combustion of these species.
- XRD data obtained with all preferred catalysts showed no evidence of phase change or segregation phenomena following their experimental evaluation towards  $\text{NO}_x$  decomposition.
- Systematic studies were performed on the three most stable catalysts, towards  $\text{NO}_x$  decomposition. In the absence of intentionally introduced hydrocarbons or other reductants into the  $\text{NO}_x$ -containing feedstream the fraction of 1000 ppm NO (in 16 percent  $\text{O}_2$ ) that was removed at a space velocity of  $50,000 \text{ h}^{-1}$  and  $500^\circ\text{C}$  ranged from 34 to 91 percent. In the simulated exhaust stream  $\text{N}_2\text{O}$  and  $\text{NO}_2$  were essentially absent as NO decomposition products. The addition of 1000ppm CO resulted in improvement in activity at temperatures above  $600^\circ\text{C}$ . Under these conditions, significant activity was obtained at  $1000^\circ\text{C}$ . Measurable activity was obtained at  $1000^\circ\text{C}$  at space velocities up to  $250,000 \text{ h}^{-1}$ .
- Preferred  $\text{NO}_x$  decomposition catalysts retained their activity when operated on-line continuously for up to 140 hours.
- Preferred  $\text{NO}_x$  decomposition catalysts demonstrated no loss of activity after exposure to 10 percent  $\text{CO}_2$  in a feed stream also containing 16 percent  $\text{O}_2$ . Tolerance to 10 ppm  $\text{SO}_2$  was also demonstrated by one catalyst (Catalyst 105).
- Two of the preferred catalysts supported on alumina and yttria- stabilized zirconia (YSZ) were prepared by incipient-wetness impregnation of those powders with solutions of the

appropriate metal nitrates.

- The effect of increased catalyst dispersion was clearly demonstrated by Catalyst 105 supported on YSZ. At a space velocity of  $1,000,000 \text{ h}^{-1}$ , this catalyst showed 35 percent removal of 477 ppm of NO in 16 percent  $\text{O}_2$ .
- Preferred catalysts were successfully incorporated onto Cordierite monoliths by introducing mixtures of the corresponding metal nitrates, followed by *in-situ* thermal processing.
- Incorporation of selected catalysts into Cordierite monoliths resulted in improved catalyst dispersion and greater (as expected specific) activity was achieved towards  $\text{NO}_x$  decomposition under net oxidizing conditions.
- Completion of Phase I resulted in the identification of catalysts possessing activity towards  $\text{NO}_x$  decomposition, under net oxidizing conditions, dramatically higher than has been previously reported. Significant progress toward meeting Air Force goals for emissions signature reduction will therefore be achieved with these materials upon completion of this overall program.

## V. ESTIMATES OF TECHNICAL FEASIBILITY

Work performed during this Phase I project clearly demonstrated that preferred catalysts can remove nitrogen oxides at conversions to  $\text{N}_2$  and  $\text{O}_2$  of 35 percent at  $10^6 \text{ h}^{-1}$ . Preliminary results showed that catalyst activity could be maintained over at least 140 hours and that the best catalyst tolerated  $\text{CO}_2$  and  $\text{SO}_2$  at levels anticipated in exhaust streams. These results point convincingly to the probable attainment of Air Force's targets of 50 percent conversion at submillisecond residence times and retention of 50 percent of initial activity after 500 hours on line.

### A) Anticipated Results

Successful completion of the overall program will result in the design and synthesis of oxygen-tolerant catalysts for the high-temperature ( $> 500^\circ\text{C}$ ) decomposition of  $\text{NO}_x$  in oxygen-rich streams. These catalysts will possess significant activities at space velocities of the order of  $> 10^6 \text{ h}^{-1}$ . The catalysts will possess thermal stability at temperatures from  $500^\circ\text{C}$  to  $1000^\circ\text{C}$ . Furthermore, the catalysts will be able to tolerate  $\text{CO}_2$ ,  $\text{SO}_2$ , and  $\text{H}_2\text{O}$ . Although the catalysts are being designed with reagentless  $\text{deNO}_x$  activity in mind, they are anticipated also to possess significant high-temperature combustion activity towards CO and unburned hydrocarbons. Consequently, catalysts developed here will reduce signatures of aircraft due to these other species as well. The catalyst will be multipurpose in character, acting to efficiently remove  $\text{NO}_x$  in the cooler regions of the engine and as a combustion catalyst in the hotter regions of the engine.

### B) Potential Use by Government

The catalysts developed in this program will find use in military aircraft of all branches of

the armed forces. Additionally, use in other gas turbine systems (e.g., in helicopters) and internal combustion engines will be attractive applications.

### C) Potential Commercial Applications

Catalysts developed here will also find use in commercial aircraft. The interest in that case would stem from Clean Air Act compliance requirements as well as potentially stricter regulations on emissions from aircraft imposed overseas and internationally. Larger potential markets are anticipated to be lean burn gasoline internal combustion engines as well as diesel engines. We have attained 91 percent conversion of NO at 400°C and 50,000 h<sup>-1</sup>, conditions appropriate to diesel engines. Both of these systems produce conditions in which oxygen is stoichiometrically in large excess over unburned fuel or incompletely oxidized species. An additional potential application is in catalytic combustion processes. Here, the goal is to burn fuel at lower temperatures, thereby reducing the thermal NO<sub>x</sub> problem. This would find application in terrestrial gas turbine systems in utility systems as well as in internal combustion engines.

### D) Significance of Anticipated Results with Regard to Phase III

Phase III commercialization will require the availability of a catalyst meeting the following requirements:

- Sufficient activity for application(s).
- Tolerance to feedstream constituents including CO<sub>2</sub>, SO<sub>2</sub>, H<sub>2</sub>O, O<sub>2</sub>, and fly ash.
- Thermal stability.

These attributes will be fully developed during Phase II. Consequently, Phase II will be necessary for the technology to be fully matured.

Both Phase II cofunding and Phase II commitments have been obtained for technology evolving in this program.

## VI. REFERENCES

1. R.K. Lyon, "New Technology for Controlling NO<sub>x</sub> from Jet Engine Test Cells," Air Force Report #ESL-TR-89-16, 1995.
2. Chemical and Engineering News, p. 34, June 30, 1997.
3. K. Tabata, J. Mat. Sci. Lett. I, 147 (1988).
4. S. Shin, Y. Hatakeyama, K. Ogawa, and K. Shmonura, Mat. Res. Bull. 14, 133 (1979).
5. C.N. Satterfield, Heterogeneous Catalysis in Industrial Practice, 2nd ed., McGraw - Hill, New York, 1991, p. 269.
6. Y. Li and W. K. Hall, J. Am. Chem. Soc., 94, 6145 (1990).
7. Y. Li, H. Dai, and Y. Lieu, New Frontiers in Catalysis, L. Gucai (Ed.), Elsevier, 1993, p. 1793.